TAMPEREEN TEKNILLINEN YLIOPISTO
TAMPERE UNIVERSITY OF TECHNOLOGY
Julkaisu 594 • Publication 594

Mari Varjonen

Three-Dimensional (3D) Digital Breast Tomosynthesis (DBT) in the Early Diagnosis and Detection of Breast Cancer

Tampere 2006

Tampereen teknillinen yliopisto. Julkaisu 594
Tampere University of Technology. Publication 594

Mari Varjonen

Three-Dimensional (3D) Digital Breast Tomosynthesis (DBT) in the Early Diagnosis and Detection of Breast Cancer

Thesis for the degree of Doctor of Technology to be presented with due permission for public examination and criticism in Rakennustalo Building, Auditorium RG202, at Tampere University of Technology, on the 12th of May 2006, at 12 noon.

Tampereen teknillinen yliopisto - Tampere University of Technology
Tampere 2006

Supervisors:
Professor Jari Hyttinen
Tampere University of Technology, Tampere, Finland.
Docent Martti Pamilo
Mammography Screening, Health Services Research Ltd; and University of Helsinki, Finland.

Reviewers:
Professor Daniel B Kopans
Harvard Medical School; and Massachusetts General Hospital, Boston, USA.
Professor Martin J Yaffe
Sunnybrook & Women's College Health Sciences Centre; and University of Toronto, Toronto, Canada.

Opponents:
Professor Peter B Dean
University of Turku; and Turku University Hospital, Turku, Finland.
Professor Daniel B Kopans
Harvard Medical School; and Massachusetts General Hospital, Boston, USA.

ISBN 952-15-1584-8 (printed)
ISBN 952-15-1585-6 (PDF)
ISSN 1459-2045

ACKNOWLEDGEMENTS

First and foremost I want to thank every woman who participated in the breast tomosynthesis study for the early diagnosis and detection of breast cancer. Without a doubt, you are the bravest group of ladies that I have ever met.

Clinical research for this thesis was conducted at the Helsinki University Central Hospital Mammography Department, Helsinki, Finland and the Jane Brattain Breast Center Park Nicollet Clinic, Minneapolis, USA from 2001-2004. I thank the caring personnel at these facilities for their understanding, help and support during this research project. Everyone was so kind and made me feel like I belonged.

While preparing my thesis, I have been employed at Instrumentarium Corporation Imaging Division, GE Healthcare and am currently working with the Planmeca Corporation Planmed Oy. I wish to express my sincere gratitude to Folke Lindberg, Juha Vanhala, Risto Luukkonen, Jean Hooks, Pekka Strömmer, Vesa Mattila, and Heikki Kyöstilä. In addition, I would like to thank all my colleagues for the amazing support you have shown; it has been great to work with you all.

My greatest gratitude and thanks goes to my principal supervisor Dr. Martti Pamilo. His guidance during this project has been invaluable. During collaboration in the collection of clinical material, he sharpened my research focus and made critical evaluations of my work when needed. His scientific experience, medical insight and help in individual publications have been most fruitful and more than essential.

My sincere thanks go to Professor Jari Hyttinen, my thesis supervisor, for his understanding, guidance, help and support. He handled many practical issues and situations so kindly, while encouraging me to finish this thesis and to continue with other new research challenges and for that I am grateful.

It is an honor to have Dr. Daniel Kopans, Director Breast Imaging Massachusetts General Hospital, and Department of Radiology Harvard Medical School, Boston, USA, as both examiner and opponent of this thesis.
It is a privilege to have Martin Yaffe, PhD from the Department of Medical Biophysics, University of Toronto, and Sunnybrook & Women's College Health Sciences Centre, Toronto, Canada, as examiner of this thesis.
It is a tribute to have Dr. Peter Dean, Chief Radiologist Breast Imaging, Turku University Hospital and Department of Diagnostic Radiology, University of Turku, Finland, as opponent of this thesis.
Dan, Martin and Peter; I am so humbled. It is with deepest gratitude that I thank each of you for the valuable time and effort that you have so willingly shared with me. I have so much respect for the valued contributions that each of you have brought to this mammography world in which we live. I have learned so much, and for that I am eternally grateful. Thank you from the bottom of my heart!

I would like to thank my Planmed colleague Ruth Grafton, for her encouragement and careful revision of my thesis. I greatly appreciate your help and I can never thank you enough. Ruth, it is my turn to say to you, *"I am going to go make me a margarita. Wish you were here!"*

I greatly acknowledge my supervisor Professor Michael Nelson, from the University of Minnesota, for our discussions, sharing your medical knowledge, and introducing me to the field of breast MRI. I appreciate your guidance and your encouraging words when most needed. I will never forget that.

I would like to take this occasion to express my gratitude to the group of medical doctors, who were involved in the collection of clinical materials. You helped me in so many ways. Thank you so much, Leena Raulisto, Marja Roiha, Mary Lechner, Eugene Elvecrog, Marco Rosselli del Turco, and Enrico Cassano. I want to take this special moment to express my gratitude to the entire group. I could not have done this without you.

I thank Rick Moore, Director of Breast Imaging Research at Massachusetts General Hospital in Boston, and medical physicists Andrew Maidment, Ann-Katherine Carton, Ehsam Samei, Tao Wu, Art Haus, Rick Webber, Barbara Lazzari, Brad Polischuk, Jerry Thomas, Hilary Alto and Jas Suri for all of your help and support, interesting discussions and significant feedback and observations. I am proud to know each and every one of you.

I am also grateful to my '3D technologists' Pirkko Kulmala, Darlene Arwidson and Kathy Wilson for helping me recognize and acquire good quality mammograms. Thank you for not giving up on me.

Lars Gunnar Månsson, Magnus Båth, Patrick Sund (Sahlgrenska University, Gothenborg, Sweden), and Markku Tapiovaara (Radiation and Nuclear Safety Authority, Helsinki, Finland) have been especially helpful in teaching, describing and giving instructions in MTF and DQE measurements.

I also would like to offer thanks to the personnel at Ragnar Granit Institute at Tampere University of Technology, special acknowledgements go to Professor Jaakko Malmivuo and Soile Lönnqvist. I am grateful to Riitta Myyryläinen from Department of Science and Engineering at Tampere University of Technology for taking her time and helping me.

A special thanks to two gentlemen, Don Blomstrom and Sergio Roncaldi, who were most helpful in arranging the clinical research sites in the United States and Italy and helping me.

I enthusiastically acknowledge the financial support received from the Finnish Cancer Organization and Instrumentarium Science Foundations. Their assistance was essential during this project.

Thanks to all my colleagues from Oy IMIX Ab; especially Matti Salmi and Eero Kettunen for introducing me to the field of medical physics in 1997-2001.

I wish to express my warmest gratitude to Professor Hannu Eskola, my Master of Science thesis examiner. The valuable instructions you gave me in 1997 prepared me for writing this doctoral thesis.

Instrumentarium Imaging had a special research and technology group; eTACT, Martti Kalke, Samuli Siltanen, Kirsi Nykänen, Juha Järvinen and Maaria Rantala, I enjoyed very much to working with you all.
Special attention goes to my colleagues Anne Aho, Arja Väyrynen, Tiina Karjalainen, and Timo Ihamäki who without hesitation regularly helped and encouraged me.
I am indebted to all my friends and family who took the time to listen, encourage and offer their guidance. During this very time consuming process, the family diversions were much needed and appreciated.

I express my warm appreciation to my parents Riitta and Jorma Lehtimäki for all their endless love, care and support. Thanks for always being there for me. I also want to thank my brother, Marko Lehtimäki for his guidance and encouragement through my lifetime.

Lastly, I can honestly say that without my beloved Vesa I would not have completed this project. I am forever thankful for all the times during this research endeavor you have shared your strength while giving me love and encouragement *to do it my own way*. You helped me so many times to find the confidence I needed to complete this project. Thanks for understanding, I love You!

Mari Varjonen

Hausjärvi, Finland
9th of April, 2006

ABSTRACT

Two-dimensional (2D) mammography plays a most important role in all aspects of breast cancer detection, diagnosis and treatment. Although it is well known that 2D mammography has limitations and it is not capable of detecting all breast cancers, there is no question that mammography is an important imaging technique for detecting and diagnosing breast cancer. Challenges of 2D mammography are structured noise which is created by the overlap of normal dense tissue structures within the breast. This may obscure the findings causing lesions to be missed (reduction of diagnostic sensitivity). Breast tissue may also simulate the presence of a cancer that does not actually exist. This causes a loss of diagnostic specificity. Currently 2D mammography is the only x-ray imaging modality accepted for breast cancer screening, but for years researchers have tried to find improved technologies and new methods to supplement 2D mammography and provide better sensitivity and specificity. Digital breast tomosynthesis (DBT) is a method that was first described many years ago, but could not be easily applied until the development of fast read-out digital detectors. The goal of breast tomosynthesis is to make available a method for screening and diagnostic mammography which provides higher sensitivity and specificity than routine mammography.

This study presents digital breast tomosynthesis in diagnostic mammography by comparing digital breast tomosynthesis and screen-film or digital mammograms clinical performance, evaluates Tuned Aperture Computed Tomography (TACT) capability as a 3D breast reconstruction algorithm in the limited angle tomosynthesis system, and demonstrates technical and clinical performance of a real-time amorphous-selenium (*a*-Se) flat-panel detector (FPD) in full field digital breast tomosynthesis.

The analyses of breast tomosynthesis have shown the following clinical benefits: improvement of overall lesion detection and analysis, increased accuracy to either confirm or exclude a suspected abnormality and in particular detection capability of small breast cancers. The results indicate that breast tomosynthesis has the potential to significantly advance diagnostic mammography, as well as screening mammography in the future. Tomosynthesis studies have already shown a promise. Based on this clinical study, tomosynthesis of the breast will increase specificity. Study also suggests that tomosynthesis might facilitate the detection of cancers at an earlier stage and a smaller size than is possible in 2D mammography.

Digital breast tomosynthesis is a new breast imaging modality which has proved to have advantages over 2D mammography. Breast tomosynthesis will lead to the earlier breast cancer detection and diagnosis and will keep the false positive rate as low as possible.

Keywords: digital breast tomosynthesis (DBT), breast cancer, three-dimensional (3D), tuned aperture computed tomography (TACT), amorphous selenium (*a*-Se), digital mammography (DM), flat panel detector (FPD)

CONTENTS

LIST OF ORIGINAL PUBLICATIONS

This thesis is based on the following publications, referred to in the text by Roman numerals.

I Lehtimäki M, Pamilo M. Clinical aspects of diagnostic 3D mammography. *Seminars in Breast Disease*. 6(2), 72-77, 2003.

II Lehtimäki M, Pamilo M, Raulisto L, Roiha M, Kalke M, Siltanen S, Ihamäki T. Evaluation clinique des performances diagnostiques de la mammography numérique avec spot et de la mammography numérique 3D suite au dépistage d'anomalies. *Le Sein.* 13(4), 309-316, 2003.

III Loustauneau V, Bissonnette M, Cadieux S, Hansroul M, Masson E, Savard S, Polischuk B, Lehtimäki M. Imaging performance of a clinical selenium flat-panel detector for advanced applications in full-field digital mammography. *Proceedings of SPIE.* 5030, 1010-1020, 2003.

IV Varjonen M, Pamilo M, Raulisto L. Combining clinical benefits of diagnostic three-dimensional digital breast tomosynthesis and ultrasound imaging. *Breast Cancer Research Journal.* Submitted for publication in November 2005. Revised in April 2006.
Varjonen M, Pamilo M, Raulisto L. Clinical benefits of combined diagnostic three-dimensional digital breast tomosynthesis and ultrasound imaging. *Proceedings of SPIE*. 5745, 562-571, 2005.

V Varjonen M, Pamilo M, Raulisto L. Digital breast tomosynthesis in diagnostic mammography. *Emerging Technologies in Breast Imaging and Mammography*. Accepted for publication and to be published in April 2006.

VI Lehtimäki M, Pamilo M, Raulisto L, Kalke M. First results with real-time selenium-based full-field digital mammography three-dimensional imaging system. *Proceedings of SPIE*. 5368, 922-929, 2004.

VII Lehtimäki M, Pamilo M, Raulisto L, Roiha M, Kalke M, Siltanen S, Ihamäki T. Diagnostic clinical benefits of digital spot and digital 3D mammography following analysis of screening findings. *Proceedings of SPIE*. 5029, 698-706, 2003.

The author's contribution to the original publications is as follows. As the first author in I, II, IV, V, VI, and VII, the author has organized the main study design, monitored the clinical research, performed data analysis, prepared the results and composed the publications. In III the author is responsible for tomosynthesis reconstruction, data analysis and results. The author participated in the design of the manuscript, and provided comments as well. Publication VII is included because publication II is written in French. Mari Lehtimäki is the maiden name of Mari Varjonen.

LIST OF ABBREVIATIONS AND SYMBOLS

2D	two-dimensional
3D	three-dimensional
ACRIN	American College of Radiology Imaging Network
ADH	atypical ductal hyperplasia
AEC	automatic exposure control
AGD	average glandular dose
ART	algebraic reconstruction technique
a-Se	amorphous selenium
a-Si	amorphous silicon
ASIC	application specific integrated circuits
BP	back projection
CAD	computer aided detection
CC	craniocaudal
CCD	charge coupled device
COG	center of gravity
CsI	cesium iodide
CT	computed tomography
DBT	digital breast tomosynthesis
DCIS	ductal carcinoma in situ
DEL	detector element
DFM	diagnostic film mammography
DM	digital mammography
DMIST	Digital Mammography Imaging Screening Trial
DQE	detective quantum efficiency
DR	digital radiography
DSI	diagnostic spot imaging, tomosynthesis two-dimensional projection images
FBD	filtered back projection
FDA	U.S. Food and Drug Administration
FFDM	full field digital mammography
FNAB	fine needle aspiration biopsy
FT	Fourier transforms
FPD	flat panel detector
GFB	gaussian frequency blending
GRE	gradient-echo
HgI_2	mercuric iodide
HRT	hormone replacement therapy
HUCH	Helsinki University Central Hospital
HVL	half-value layer
IEC	International Electrotechnical Commission
LCIS	lobular carcinoma in situ
LM	lateromedial
LSA	linear-system analysis

LSF	line spread function
LST	linear-systems theory
MIP	maximum intensity projection
MITS	matrix inversion tomosynthesis
ML	iterative maximum-likelihood algorithm
MLO	mediolateral oblique
Mo/Mo	molybdenum target and molybdenum filters
MRI	magnetic resonance imaging
MTF	modulation transfer function
MTF_{pre}	presampling modulation transfer function
NCI	National Cancer Institute
NEQ	noise equivalent quanta
NIH	National Institutes of Health
NNPS	normalized noise power spectrum
NPS	noise power spectrum
PAD	pathological anatomy diagnosis
PbI_2	lead iodide
PET	positron emission tomography
PMMA	polymethyl methacrylate
ROC	receiver-operating characteristic
ROI	region of interest
S	average signal response measured on the gain and offset corrected data
SAA	shift-and-add
SFM	screen-film mammography
SNR	signal-to-noise ratio
TAB	tape-automated bonding
TACT	tuned aperture computed tomography; a registered trademark of Wake Forest University
TDLU	terminal ductal-lobular unit
TFT	thin-film transistor
US	ultrasonography

1 INTRODUCTION

Breast cancer is one of the most common malignancies in the female population. Mammography has been the most effective technique for early detection and diagnosis of breast cancer. Breast cancer screening has led to a substantial reduction in breast cancer mortality during the past 20 years[15, 31 116, 117]. This mortality reduction is an important step toward lessening the burden of breast cancer, but most breast imaging experts acknowledge the limitations of mammography screening, especially in women with dense breasts[42]. Challenges of two-dimensional (2D) mammography are limited sensitivity, superimposed normal breast tissue which may obscure a finding, or superimposed tissue that may look like a cancerous lesion, dense breast tissue, and structured noise which is created by the overlapping of normal structures within the breast. Anatomy of the human breast is explained in figure 1.
Figure 2 shows an example of screening mammogram images, mediolateral oblique (MLO) and craniocaudal (CC) views.
Recall rates refer to the percentage of women asked to return for additional imaging work-up after batch interpretation of their screening mammogram. Batch interpretation can be performed successfully only if recall rates are maintained within acceptable limits. Recall rates that are too high can cause women inconvenience, anxiety and result in increased cost and inefficiency of the screening process. If however recall rates are too low, some subtle cancers may be missed and some benign lesions may undergo unnecessary biopsy because

supplementary views and ultrasound that could have provided definitive evaluation of screen-detected findings were not performed[21].

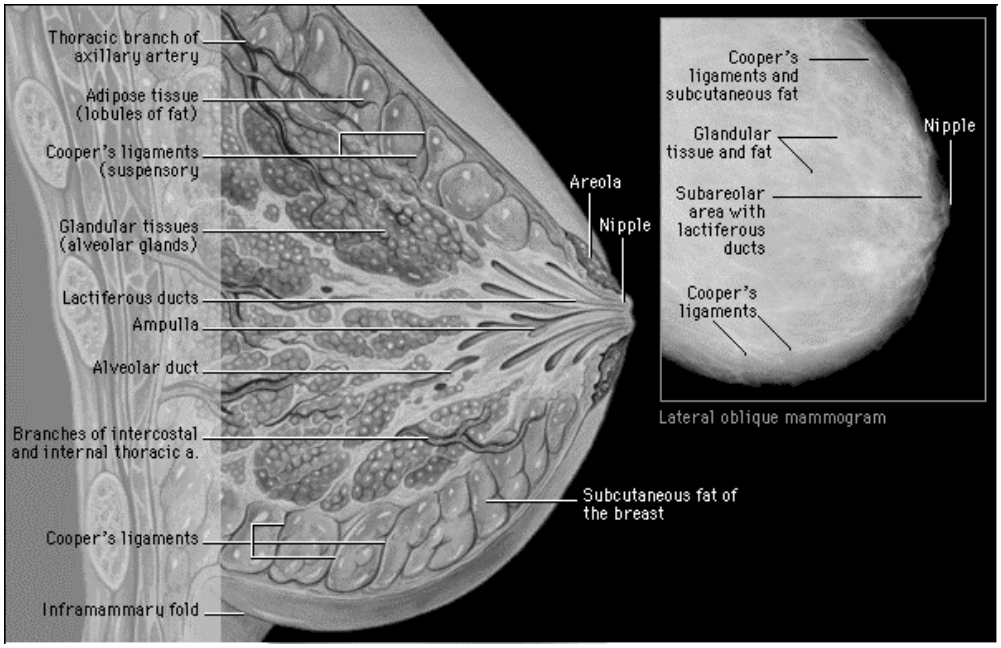

Figure 1. Anatomy of the breast (Copyright: 2004, Yale University School of Medicine). Each breast has 15 to 25 sections, called lobes or segments. Each lobe is defined by a branching network of lactiferous duct that conduct milk to the nipple from the lobulus where it is produced. The main collecting ducts open on the surface of the nipple. The glandular tissues of the breast are the terminal duct lobular units (TDLU) which form the basic functional unit of the breast. The TDLU is composed of a small segment of terminal duct and a cluster of ductules or acini in which milk is secreted during lactation. Fat and fibrosis connective tissue fills the spaces between lobules and ducts. The lymph vessels in the breast lead to small organs called lymph nodes. The most important lymphatic drainage is to the axilla, while less of the lymph flow is drained via internal mammary and posterior intercostal lymphatics.

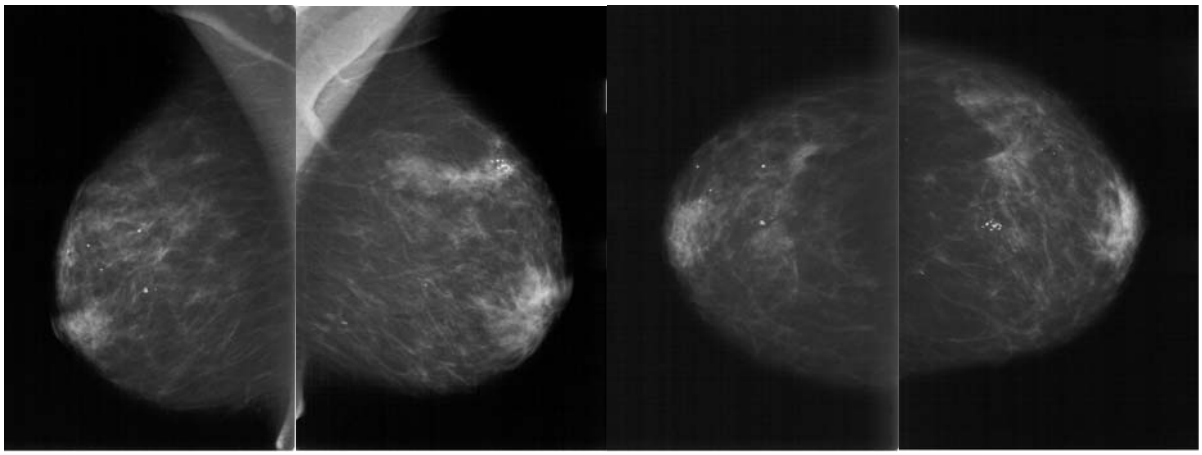

Figure 2. Screening mammograms of a 54-year-old woman: mediolateral oblique (MLO) and craniocaudal (CC) views.

Mammographic findings are nonspecific in many cases, and the nature of the detected lesion cannot be fully revealed. Some lesions may be obscured due to dense parenchyma or be impossible to differentiate from normal or benign structures. In these cases, adjunctive methods are needed[95]. Conventional mammography and ultrasound are the primary imaging methods. Limitations in sensitivity and specificity continue to prompt investigation into new imaging methods.

Technological improvements have included the development of dedicated digital mammography systems called full field digital mammography (FFDM) which is a relatively new technology. Digital mammography will be reviewed later in Chapter 2.

Ultrasound (US) is well accepted as the most useful adjunct to mammography for the diagnosis of breast abnormalities. US is most often used to assess palpable masses and non-palpable masses that have been detected during screening mammography[3, 17, 24, 42]. US may demonstrate malignancies and other masses, which are not visible mammographically. Recently the utility of current state-of-the-art breast US has been evaluated as a screening examination for breast cancer, as a way to stage disease pre-operatively and guide treatment in patients recently diagnosed with breast cancer, and as a means to discriminate between benign and malignant solid lesions. Multiple enhancements – including improved probe technology, organ-specific software algorithms, and increased computing power – have led to better spatial and contrast resolution and therefore better imaging capability. It is not surprising that US can detect cancers that are both mammographically occult and too small to be palpable[29]. Studies have proven that US has been found to be a valuable adjunct to mammography for characterizing breast lesions as cysts and solid masses and evaluating palpable masses that are obscured by dense breast tissue on mammograms[3, 42]. As an ultrasound wave propagates through tissue at high amplitudes, spatial compounding, also referred to as cross-beam imaging, is the combination of images or image scan lines acquired from multiple angles[24]. Examples of ultrasound images are shown in figures 3 and 4.

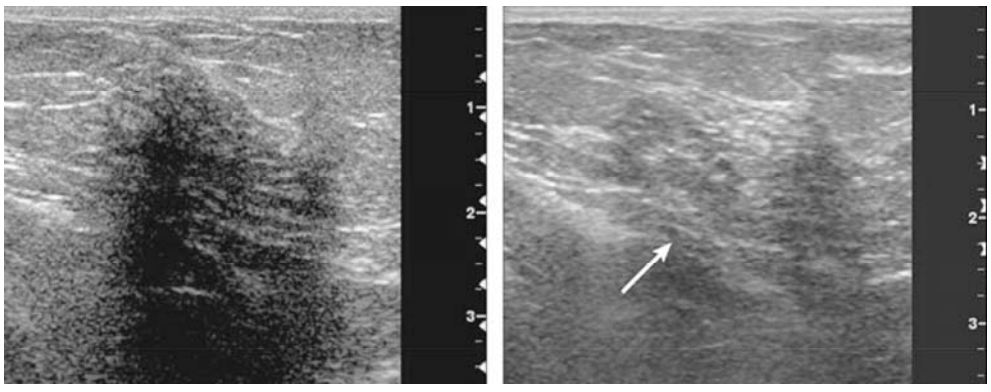

Figure 3. Single-sweep and cross-beam (compound) US images of 1.6 cm infiltrating ductal carcinoma in a 44-year-old woman with invasive lobular carcinoma. Cross-beam image shows more complete tumor borders, particularly posterior borders (arrow), at least for the major tumor on the left. In the cross-beam image, more echogenic in-homogeneities are seen in the tumor, and connective tissue planes are seen more completely. (Copyright: Carson PL, LeCarpentier GL, Roubidoux MA, Erkamp RQ, Fowlkes JB, Goodsitt MM. Physics and technology of breast US imaging including automated three-dimensional US. RSNA Categorical Course in Diagnostic Radiology Physics: Advances in Breast Imaging-Physics, Technology, and Clinical Applications 2004; 223-232).

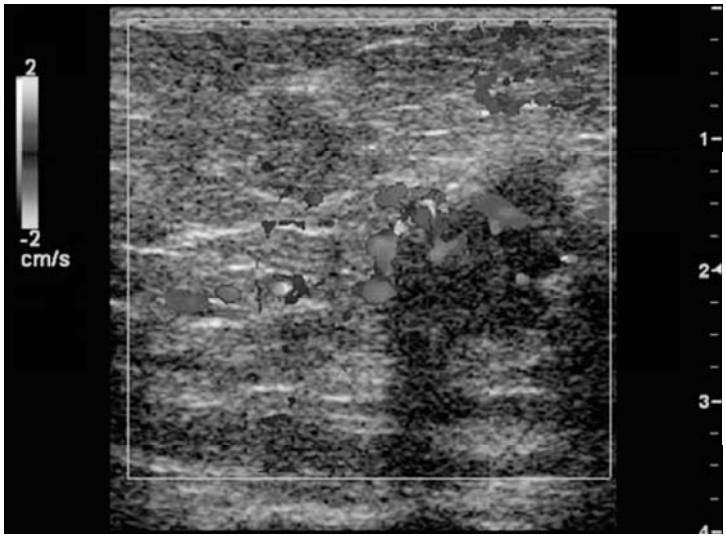

Figure 4. Color Doppler flow image of the same 1.6 mm infiltrating ductal carcinoma shown in figure 3. Extensive vascularity is seen around lesion and penetrating into it. (Copyright: Carson PL, LeCarpentier GL, Roubidoux MA, Erkamp RQ, Fowlkes JB, Goodsitt MM. Physics and technology of breast US imaging including automated three-dimensional US. RSNA Categorical Course in Diagnostic Radiology Physics: Advances in Breast Imaging-Physics, Technology, and Clinical Applications 2004; 223-232).

Earlier efforts at US scanning in a mammographic view did not address the use of many advanced US imaging techniques that are beginning to show potential for the detection and diagnosis of breast cancer[10]. One of the promising new approaches is the simultaneous acquisition of tomosynthesis images with ultrasound images of the breast. This would permit the fusion of US and full field digital mammography (FFDM) image information to improve diagnostic accuracy. A patient image is shown in figure 5.
With this system, positioning of the breast in exactly the same orientation as that of a particular mammogram and identifying structures between the two modalities should be much improved over what is possible with hand scanning even by the most skilled professionals. Another ongoing effort is building a prototype designed for limited-field digital mammography stereotactic biopsy. In this system, the US transducer moves alongside the scanning slit digital detector[10].

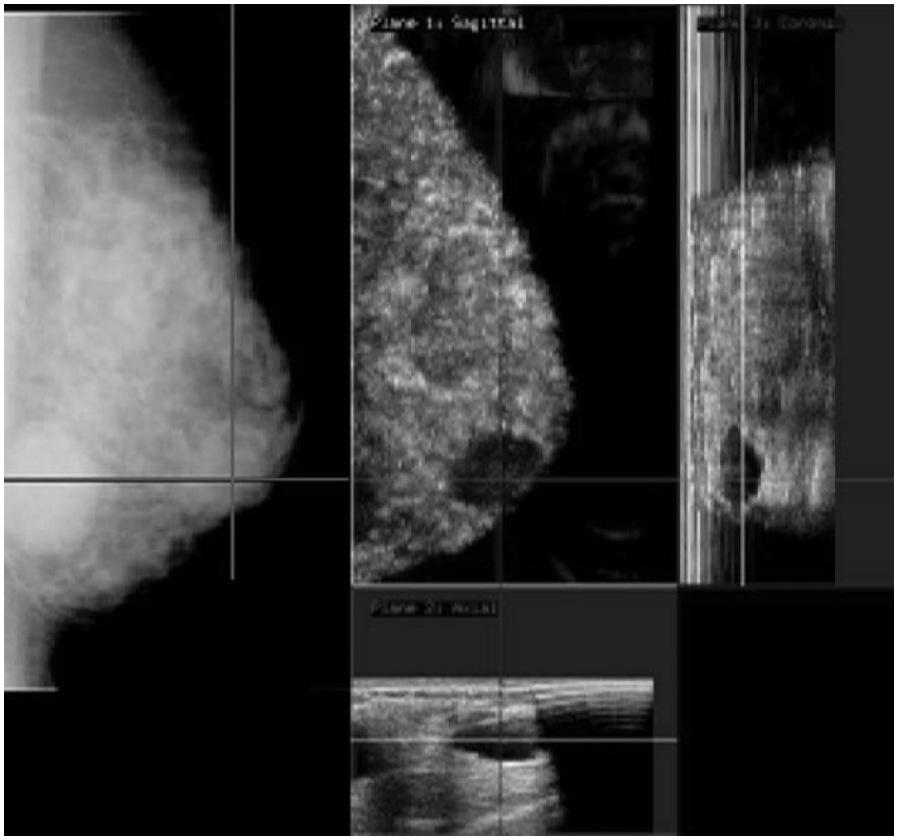

Figure 5. Co-registered lateral-medial images of right breast of a 52-year-old woman with multiple breast cysts (Copyright: Carson PL, LeCarpentier GL, Roubidoux MA, Erkamp RQ, Fowlkes JB, Goodsitt MM. Physics and technology of breast US imaging including automated three-dimensional US. RSNA Categorical Course in Diagnostic Radiology Physics: Advances in Breast Imaging-Physics, Technology, and Clinical Applications 2004; 223-232).

Breast magnetic resonance (MR) imaging has gained acceptance as an important complementary diagnostic method for use in the evaluation of breast disease[18, 22, 35, 52]. MR imaging has now emerged as a promising new modality for the detection, diagnosing, and staging of breast cancer[22, 44, 64]. The higher soft-tissue contrast and gadolinium-enhanced techniques available with MR imaging allow the detection of cancers that are clinically, mammographically, and sonographically occult. Breast MR imaging is emerging today as a promising adjunctive imaging modality. Its advantages include the absence of ionizing radiation and the ability to depict cancers that are not visible with other imaging methods. It is generally agreed that MR imaging is probably the study of choice for evaluating the integrity of implants. MR imaging is now used with increasing frequency to evaluate patients before and after treatment for breast cancer. Investigations have shown that MR imaging can be used to detect invasive breast cancer with high sensitivity. MR imaging examinations of the breasts are currently performed with a wide variety of techniques, coils, and field strengths. The true sensitivity of MR imaging is not yet known, because large clinical trials would be needed to establish its sensitivity in cancer screening. Imaging protocols, along with post-processing techniques and biopsy systems are currently undergoing evaluation. The

cost-effectiveness of MR imaging needs further study, and a cost-benefit analysis will be necessary before breast MR imaging examinations become uniformly reimbursable[34, 43, 78, 113]. Kriege, Warner and Leach have done a lot research and demonstrated importance in use of MRI in screening women at high genetic risk.

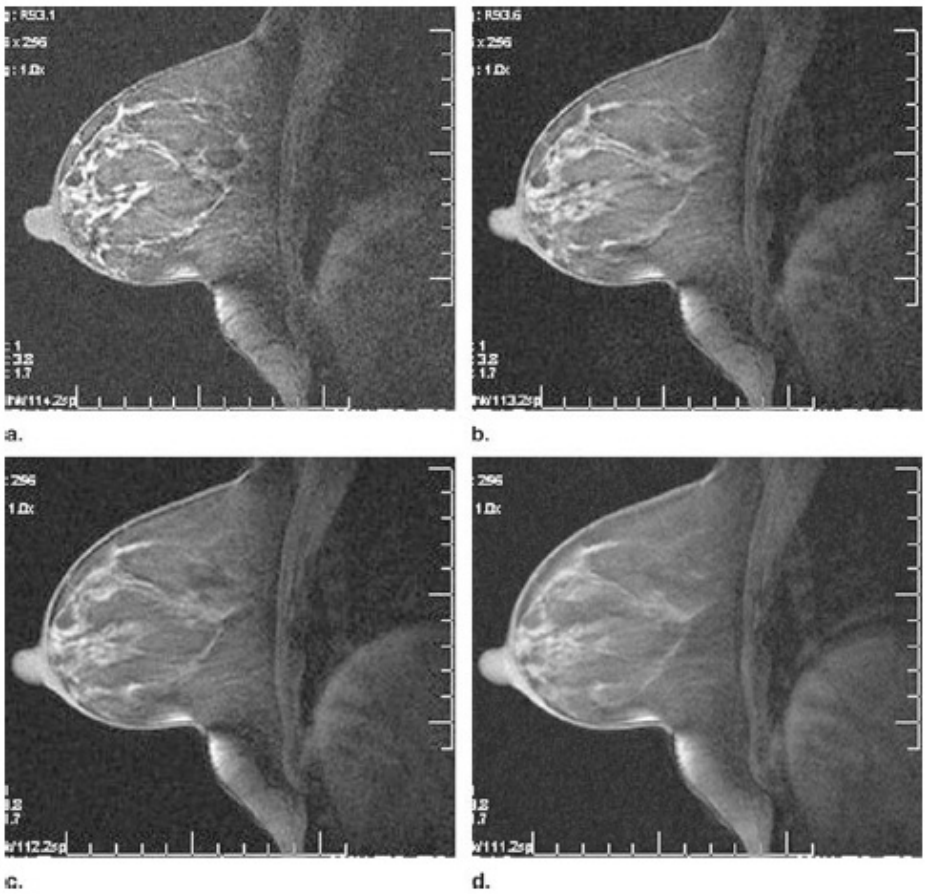

Figure 6. Example of gradient-echo (GRE) MR images showing effect of section thickness on tissue visibility with sections of 1 mm, 2 mm, 3 mm, and 4 mm (Copyright: Hendrick RE. Physics and technical aspects of breast MR imaging. RSNA Categorical Course in Diagnostic Radiology Physics: Advances in Breast Imaging-Physics, Technology, and Clinical Applications 2004; 259-278).

There is lot of other development going on in the area of breast imaging; elasticity imaging, and molecular imaging (fluorodeoxyglucose positron emission tomography (PET), mammoscintigraphy, and sentinel lymph node techniques). Digital mammography itself provides new possibilities and techniques. Three areas of potential improvement over conventional 2D mammography are dual-energy subtraction, contrast subtraction, and digital breast tomosynthesis. Digital breast tomosynthesis is introduced in Chapter 2.
Although clinical trials of digital breast tomosynthesis have only begun, initial evaluation suggests the following benefits of tomosynthesis compared with conventional mammography:

1. enhanced lesion visibility
2. superior analysis of lesion margins
3. reduction in the number of false-positive findings through elimination of overlapping structures
4. precise lesion localization through three-dimensional data acquisition
5. imaging in a single compression
6. imaging each breast at a radiation dose less than that used for conventional mammography[49, 79, 80, 90, 91, 92, 93, 94, 136].

The purpose of this thesis is to prove that digital breast tomosynthesis has the potential to provide clinically important information which cannot be obtained with conventional breast imaging methods. Three-dimensional (3D) digital breast tomosynthesis seeks to (1) determine whether a mammographic finding is the result of a 'real' lesion or the superimposition of normal parenchyma structures, (2) detect subtle changes in breast tissue, which might otherwise be missed, and (3) to reduce the number of biopsies performed by reducing the need for biopsy by permitting more accurate differentiation between benign and malignant lesions and (4) verify the correct biopsy target if the procedure is needed.
The study was designed to compare clinical benefits either of the standard screen-film mammograms, or digital mammograms to digital breast tomosynthesis based on sensitivity and specificity. Another goal was to evaluate and demonstrate the performance of real-time selenium-technology-based full field digital mammography (FFDM) system in breast tomosynthesis. The coordinated goal was to evaluate and determine clinical benefits when a Tuned Aperture Computer Tomography (TACT) reconstruction algorithm is used in digital breast tomosynthesis for early diagnosis and detection of breast cancer.
Objectives of the study will be summarized in more detail in Chapter 3. Chapter 2 includes a review of the literature, as an introduction to the motivation for 3D imaging of the breast, a description of the current approaches and an introduction to the tools used for quantitative image analysis. Chapter 4 presents the methods and materials for the clinical research and Chapter 5 summarizes the technical evaluation methods for full field tomosynthesis. The clinical results are presented in Chapter 6 and technical performance in Chapter 7. Finally, Chapter 8 summarizes the further work and challenges in the early detection and diagnosis of breast cancer.

2 SCIENTIFIC AND TECHNICAL BACKGROUND

Today most clinical x-ray imaging of the breast is performed with screen-film mammography (SFM) technique because of the high spatial resolution (18-20 line pairs per millimeter) and contrast requirements of mammography. There are some limitations of SFM associated with its limited dynamic range and contrast characteristics, which often make detection of low-contrast features, such as masses and architectural distortion difficult[82]. Full field digital mammography (FFDM) offers potential improvements over the limitations of SFM[114]. The recently completed Digital Mammography Imaging Screening Trial (DMIST) showed the overall diagnostic accuracy of digital and film mammography as a means of screening breast cancer is similar, but digital mammography is more accurate in women under the age of 50 years, women with radiographically dense breasts, and premenopausal or perimenopausal women[86]. Although, the sensitivity is lower the authors would like to have. Based on this study about 20%-30% breast cancers were missed[86].

One benefit of using digital mammography at the present time comes from more reliable and efficient image management. The main benefit of developing digital mammographic systems is the fact that they open important new avenues of exploration for using x-rays to image the breast. Digital x-ray imaging offers a great opportunity to improve one's ability to detect and diagnose more breast cancers earlier. One of the potential improvement areas is three-dimensional (3D) mammography, digital breast tomosynthesis (DBT)[49].

2.1 Basics of digital mammography

In digital mammography, the screen-film system is replaced by a detector, which produces an electronic signal that is digitized and stored. The detector is designed to provide a signal which is highly linear (or logarithmic) with radiation intensity and where the response does not flatten out at low or high intensities. Digital images are sampled images. These are defined by the size of the detector element (del). Each element has finite set of values ranging from 0 to 2^n-1, where n is the number of bits of digitization. The precision of image recording is determined in part by the number of bits. For example, a 12-bit system represents signal levels from 0 to 4095. In such a system, if the actual signal presented by the detector corresponded, for example, to 1203.5, it would be represented as either 1203 or 1204 because 1203.5 do not exist. To gain such precision, a 13-bit system would be required, in which case, the signal would appear as 2407 on a scale from 0 to 8191. Another difference between analog and digital mammography relates to image noise. As in SFM, image fluctuation is determined both by the number of x-rays that strike the detector (known as the quantum fluctuation) and also the inherent granularity of the detector. In SFM the film itself has a granular structure, which is unique to each sheet of film and, therefore, cannot be removed from the image. In most digital mammography systems, the same detector is used repeatedly. Therefore, any structure noise can be recorded and used as a correction mask to remove the effect of this fixed pattern noise from subsequent images[138].

2.1.1 Detectors for digital mammography

Digital detectors create an electronic image of the imaged structure as picture elements, pixels. These images may be captured by the detectors indirectly by using an x-ray scintillator, which first emits light and then produces an electronic image on the digital detectors. The detectors used for this approach are typically amorphous silicon (*a*-Si) flat panels or charge-couple-devices (CCDs). This is identical to what happens with SFM except that the detector is film instead of a digital device. The image may also be captured by the digital detector directly without using a scintillator. In this case, x-rays produce the latent electronic image by direct interaction with a photoconductor detector. The detectors used for this approach are typically amorphous selenium (*a*-Se) flat panels. Figure 7 provides information about some commercially available flat-panel detector (FPD) systems in digital radiography (DR). The development of DR detectors can be divided in two areas: the development and optimization of the x-ray detection materials and the improvement of the flat-panel arrays itself. Research into new and improved x-ray materials has been on going for many years. Lead iodide (PbI_2) and mercuric iodide (HgI_2) have been reported in the literature[139].

2.1.2 Imaging performance

It is important to realize that the value recorded by the acquisition system for each pixel is a combination of the signal and noise[138]. The requirements for an imaging system and the demands on the image quality are dependent on the imaging task. However, a desire to describe the imaging properties of an imaging system in an objective way, without taking the

specific imaging task into account, has led to the application of linear-systems analysis (LSA) to medical imaging systems. LSA, based on linear-systems theory (LST), can be used to give measures of the ability of the system to pass a signal, as well as of the noise characteristics of the system[12].

When evaluating system performance, the following quantities are important:

1. Modulation Transfer Function (MTF), describing the signal transfer in the system as a function of spatial frequency. A transfer function curve that plots the modulation of a signal versus spatial frequency. Signal blurring caused by light spread in a phosphor causes an increasing loss of modulation with increasing spatial frequency, depicted by the MTF curve. Line Spread Function (LSF) and MTF are related to each other by a process known as Fourier transformation.

2. Noise Power Spectrum (NPS), giving a detailed description of the noise of the system. A spectrum of the noise contributions as a function of spatial frequency of the detector arising from quantum, electronic and fixed pattern noise sources.

3. Detective Quantum Efficiency (DQE), describing the efficiency of the system in transferring information. A measure of the efficiency of information transfer, measured as a ratio of the ideal observer's (signal to noise ratio)^2 in the image relative to the ideal observer's (signal to noise ratio)^2 of the incident radiation signal. The DQE(f) of a detector is calculated as a function of spatial frequency using MTF and NPS measurements as well as incident radiation fluency.

$$DQE(u,D) = \frac{MTF(u)^2}{NNPS(u,D) \times SNR(D)^2}.$$

Where u and D are spatial frequency and dose respectively, MTF is the Modulation Transfer Function and NNPS is the Normalized Noise Power Spectrum, i.e. NPS divided by the large area signal in the image used for the NPS calculation. SNR is the Signal-to-Noise Ratio of the incoming radiation.

4. Signal-to-Noise Ratio (SNR), describing the peak signal to the source of the noise in the background; this is different than contrast-to-noise or detail signal-to-noise ratios, which represent the difference of the signal and the background divided by the source of the noise in the background.

$$SNR^2 = \frac{\left(\int q(E) \times E \, dE\right)^2}{\int q(E) \times E^2 \, dE}.$$

Where q(E) is the number of photons with energy E.

Array/ Detector Manufacturer.	Product Family	Size¶ (cm)	Pixel Pitch (μm)	No. of Pixels	X-ray Absorbing Material‡	Pixel Components #
a-Si:H Flat-panel Systems (Indirect)						
General Electric/ Perkin Elmer	Revolution XQ/I, XR/d™	41x41	200	2048x2048	CsI:Tl undisclosed thickness	a-Si:H nip photodiode + TFT switch
	Innova 4100™					
	Senographe 2000D™	18x23	100	1800x2304		
Trixell	Pixium 4600™ Siemens: Thorax/Vertix/Multix™ FD, Axoim Aristos™ FX Philips:Digital Diagnost™ Infimed & Listem: Stingray DR™	43x43	143	3121x3121	CsI:Tl ~550μm	a-Si:H nip photodiode + switching diode
	Pixium 4800™ Philips: Integris Allura™ 9	25 diagonal.	184	960x960	CsI:Tl ~550μm	a-Si:H nip photodiode + TFT switch
Varian/ dpiX	PaxScan™ 2520 Hitachi*	20x25	127	1536x1920	Gd_2O_2S:Tb or CsI:Tl ~600μm	a-Si:H nip photodiode + TFT switch
	PaxScan™ 4030A/R Hitachi: FPD-DR*	30x40	194	1536x2048		
Canon	Canon: CXDI™ 40G Agfa: ADR Thorax™	43x43	160	2688x2688	Gd_2O_2S:Tb ~200μm	MIS photodiode + TFT switch
	Canon CXDI™ 50G (portable)	35x43		2208x2688		
	Canon CXDI™ 31 (portable)	23x29	100	2256x2878		
a-Si:H Flat-panel Systems (Direct)						
Direct Radiography Corp.	Hologic: Epex, Radex™ Eastman Kodak:DirectViewDR™. Fischer Imaging: VersaRad D™	35x43	139	2560x3072	a-Se ~500μm (dielectric HV protection layer)	Storage capacitor + TFT switch
	Lorad: Selenia™ Agfa: Embrace™ Siemens: FFDM-FD™	25x29	70	3584x4096	a-Se ~250μm (dielectric HV protection layer)	
Anrad Corp.	Toshiba: DynaDirect™*	22x21	150	1460x1440	a-Se ~1000μm (p-i-n HV protection layer)	Storage capacitor + TFT switch
		35x35		2304x2304		
	Instrumentarium: Diamond DX™*	18x24	85	2816x2048	a-Se ~200μm (p-i-n HV protection layer)	
Sharp	Shimadzu*	23x23	150	1536x1536	a-Se ~1000μm (also CdZnTe)	Storage capacitor + TFT switch
CCD Based Systems						
SwissRay	ddR™ systems	35x43	167	~2500x2000	CsI, undisclosed doping	4 overlapping CCDs
Wuestec	DX2000™	35x43	120	3072 x 3895	Gd_2O_2S:Tb	Single CCD
Imaging Dynamics	Xplorer 1700™	43x43	108	~4000x4000	Gd_2O_2S:Tb	Single CCD
Oy ImixAB	Imix 2000™	40x40	200	2000x2000	Gd_2O_2S:Eu	Single CCD
Fischer Imaging	SensoScan TrueView™	21x29	54	4096x5624	CsI:Tl	Line scanned TDI CCD
Delft Diagnostic Imaging	Thorascan™	44x44	162	2736x2736	CsI:Tl ~500μm	Line scanned TDI CCD
Cares Built	Clarity 7000™	43x43	60	7000x7000	Gd_2O_2S:Tb	20x20 CMOS array
Star V-Ray	Tradix 4000™	43x43	140	3080x3080	Gd_2O_2S:Tb	8x8 CMOS array
Other Systems						
Sectra Imtec AB	MDM™* (MicroDose Mammography)	24x26	50	not available	10mm thick crystalline silicon	Line scanned Photon counting
Edge Medical	Quix™* DR systems	43x43	120	3420x3420	a-Se, undisclosed thickness	Mechanically scanned line readout

Figure 7. Commercially available detector systems (Copyright: Yorkston J. Digital radiography technology. Advances in Digital Radiography: RSNA Categorical Course in Diagnostic Radiology Physics 2003; 23-36). Table of commercially available detector systems was up to date in early 2004, and there is continuous development and changes. For example three manufactures in digital mammography are not listed in this table: Planmed Oy, XCounter and IMS Giotto.

2.2 Digital breast tomosynthesis (DBT)

The ability to produce tomographic sections through the body with x-rays to eliminate structured noise was developed decades ago. In the late 1970's, linear and polycycloidal tomography was used to evaluate many organ systems. During exposures that lasted several seconds, the x-ray tube was moved in one direction while the film receptor was moved in the opposite direction. Only structures in the plane of interest stayed perfectly aligned and in sharp detail during the exposure, while structures that were out the plane on interest were blurred by the motion. Only the structures at the fulcrum of movement stayed registered. To see another plane, the fulcrum of the motion was shifted, and another exposure was made. Commonly used to evaluate other organ systems, such as kidney and chest, this technique was not feasible for breast evaluation[49]. Breast tomosynthesis acquires multiple images as the x-ray source moves through an arc above the stationary compressed breast and digital imaging detector. As the acquisition begins, the beam moves through a series of positions in different degrees. Once the projections of the breast are obtained during a tomosynthesis sequency, they can be reconstructed into a data set of slices through the breast in planes parallel to the detector and displayed in a manner suitable for review by a radiologist[58, 89]. In this way all slices through the breast can be obtained from a limited number of exposures and each exposure need only be a fraction of a full mammographic exposure so that the total dose can be within that used for standard 2D mammography screening.

2.2.1 Prototypes of digital breast tomosynthesis units

Two major breast tomosynthesis prototype systems were introduced in 1998-2001. Diamond Delta 32 TACT (Instrumentarium Corporation now part of GE Healthcare) is still the only one having 510(k) clearances for diagnostic breast tomosynthesis. This system incorporates a CCD small-area detector with 48μm pixel size, and is using TACT 3D technology, in figure 8. The only whole-breast digital breast tomosynthesis system was developed at Massachusetts General Hospital, Boston, in conjunction with General Electric with support from Department of Defense (IDEA DAMD-97-1-7144 and CTR DAMD 17-98-8309). This prototype tomosynthesis system uses a FFDM detector consisting of cesium iodide (CsI) scintillator directly deposited on an amorphous silicon (*a*-Si) transistor-photodiode array. The in plane resolution of the system is that of the detector, in this case 100 μm[92].
In 2003, the capability of real-time selenium-technology based FFDM system for breast tomosynthesis was evaluated. The prototype, Diamond DX (Instrumentarium Corporation now part of GE Healthcare) FFDM system, figure 8, was used in the evaluation. Today more prototypes of whole-breast tomosynthesis have been introduced by Planmed (based on *a*-Se technology), GE Healthcare (based on *a*-Si technology), Siemens (based on *a*-Se technology), Hologic (based on *a*-Se technology) and XCounter (based on photon counting technology).

2.2.2 Principle of breast tomosynthesis

With stereotactic tubehead movement, the digital mammography system acquires a number of projection images with different angles, shown in figure 9. The total arc varies between 30˚ to 60˚. The number of projection images varies from 7 to 25 exposures. The patient is

seated during the tomosynthesis study since the complete set of exposures must be accomplished with the breast held in compression while the patient remains motionless. The time of complete acquisition varies from 8 to 90 seconds. After each exposure, the tube moves to the next position and stops to acquire the next image. The projection images obtained during a tomosynthesis sequence must be reconstructed. As the x-ray source moves along an arc above the breast, algorithms allow reconstruction of arbitrary planes in the breast from limited-angle series of projections. Almost every research group has their own specific way to perform a tomosynthesis study. Many important parameters for breast tomosynthesis have an effect on quality of 3D data, and are currently under evaluation among many research groups:

- Number of projection images
- Total dose of the tomosynthesis study
- Slice 'thickness'
- Number of slices
- Type of detector technology
- Type of detector motion (continuous, step and shoot)
- Radiation source (tube voltage and current, filtering)
- Quality of x-ray beam
- X-ray tube (choice of the anode target material, focus spot)
- Acquisition time
- Detector calibration
- Reconstruction time
- 3D data visualization (slices, 3D volume model, slab)
- 3D workstation
- Compression force
- Reconstruction algorithms
- Post-processing (image enhancement, maximum intensity projection MIP)
- Algorithm development of gridless full field digital mammography
- Angle dependent projection image pre-processing

The following reconstruction algorithms have studies in breast tomosynthesis:

- Shift-and-add SAA
- Tuned Aperture Computed Tomography TACT
- Back Projection BP
- Filtered Back Projection FBP
- Iterative Matrix Inversion Tomosynthesis MITS
- Maximum-Likelihood Algorithm ML
- Algebraic Reconstruction Technique ART
- Gaussian Frequency Blending GFB.

FBP is a Fourier-based algorithm. Reconstruction of breast tomosynthesis projections with a filtered back projection technique achieves the goal of eliminating structure overlap that can obscure lesion margins. Chen et al have investigated a lot of digital breast tomosynthesis reconstruction algorithms. They have studied that MITS shows better high frequency response in removing out-of-plane blur, while FBP shows better low frequency noise prosperities. GFB showed more low frequency breast tissue content. They have not noticed substantial difference for SAA and FBP. SAA and TACT tomosynthesis reconstruction algorithm are a typical and fast mathematical methods. Wu et al have developed ML method. The maximum likelihood solution is the reconstructed volume that maximizes the probability of the measured projections. The advantage of this iterative method compared with FBP reconstruction is that information about the object itself can be incorporated into the reconstruction in the form of constraints[89, 137].

Figure 8. On the left side Diamond Delta 32 for diagnostic breast tomosynthesis system. This system incorporates a CCD small-area detector with 48 μm pixel size, and is using TACT 3D technology. On the right side the prototype of tomosynthesis FFDM system (Diamond DX) based on *a*-Se technology with 85 μm pixel size.

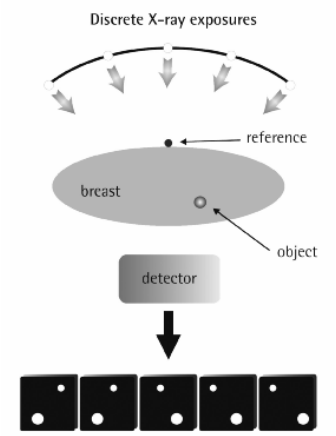

Figure 9. Principle of breast tomosynthesis imaging
(Copyright Timo Ihamäki).

2.3 Breast computed tomography (CT)

In response to the demand for more sensitive breast cancer detection, several research groups in North America have been interested in the development of dedicated breast computed tomography (CT) and its efficacy in the early detection of breast cancer[7, 28, 73, 81, 99, 119, 122]. The x-ray tube and flat-panel detector system are mounted on a conventional CT gantry and rotate in a horizontal plane[7]. Limited-angle tomography, breast tomosynthesis has been studied. The tomosynthesis approach is similar to that of geometric tomography. The trade-offs between digital breast tomosynthesis and breast CT will need to be evaluated when more in known about both techniques.

In practical terms in breast CT requirements are that both the detector and x-ray tube need to rotate just below the patient table with very close tolerances. This implies that the x-ray tube should have its focal spot positioned near the physical end of the tube and that the detector should have very little dead space near its top edge. A full cone-beam CT scanner is the epitome of multi-detector row CT; one revolution of the source and detector permits acquisition of all information needed to reconstruct all of the required CT sections. Cone-beam CT scanners require different reconstruction algorithms than those for conventional fan-beam commercial scanners, but as state-of-art commercial CT scanners extent beyond 16 detectors, they also employ cone-beam reconstruction techniques. The maximum cone angle is about 25˚ with the geometry defined in figure 10. This large cone angle will likely be a source of artifacts near the nipple end of larger breast images. Ultimately full cone-beam acquisition and reconstruction may not be consistent with optimal image quality in breast CT. If that proves true, then limited cone-angle multiple-rotation technique will become necessary. Such systems will require more mechanical complexity and will likely be a challenge to construct in an academic setting. Until clinical trials are performed, the role of breast CT in breast cancer detection and diagnosis remains an exciting but unproved possibility[7, 81].

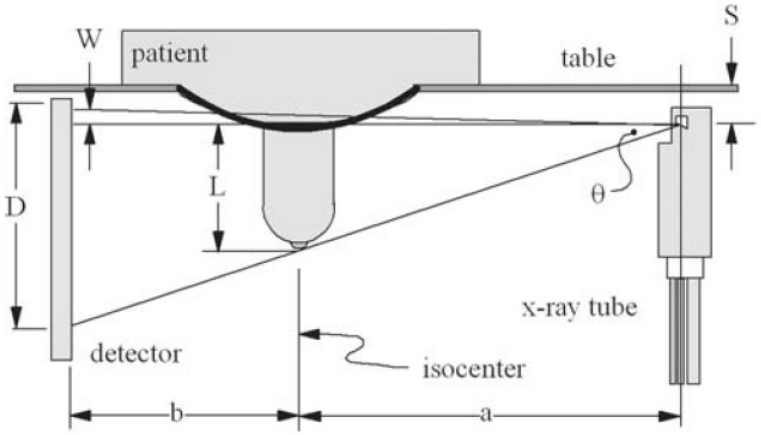

Figure 10. Diagram shows geometry of a breast CT scanner. a = source-to-isocenter distance, b = isocenter-to-detector distance, D = height of breast image in detector plane, L = length of breast, S = distance between bottom of table and x-ray focal spot, W = length of breast above the central ray, and θ = cone angle (Copyright: Boone JM. Breast CT: Its prospect for breast cancer screening and diagnosis. RSNA Categorical Course in Diagnostic Radiology Physics: Advances in Breast Imaging-Physics, Technology, and Clinical Applications 2004; 165-177).

2.4 Advanced applications in digital mammography

Because digital mammography offers the potential for improved clinical methods in breast imaging, many advanced applications are under development. Of course all new applications need to be evaluated properly, concentrating on proving clinical success in the sense of increased sensitivity and specificity with lower cost of workflow and reduced risk. Important aspects in defining the efficacy of a test is its ability to either confirm or exclude a suspected abnormality, its associated risk, discomfort, or inconvenience. As mentioned before, three of the areas of potential improvement are dual-energy subtraction, contrast subtraction, and digital breast tomosynthesis[49, 79, 80].

2.4.1 Dual-energy imaging

The detection of clustered micro-calcifications is one of the advantages of x-ray mammography. One way is to make calcifications stand out through the use of dual-energy subtraction[49]. The dual energy technique makes use of the physics of x-ray interaction with matter to distinguish objects with different element compositions[1, 13, 40, 48, 51, 59, 111, 112, 123]. X-ray quanta interact with matter in the energy range of diagnostic imaging by two primary processes: Compton scattering and photo electronic absorption. Compton scattering involves the scattering of a photon off a loosely bound electron and results in scatter radiation commonly known in radiography, as well as some energy deposition in the tissue. Photo electronic absorption occurs when an incident photon ejects an electron from an atom. Because these two processes depend on different interactions between photons with matter, it is not surprising that their dependence on the energy of the incident photon differs. Compton scattering is only slightly dependent on the energy as the photon increases. Figure 11 shows the different energy dependence of soft tissue and bone[1, 13, 123].

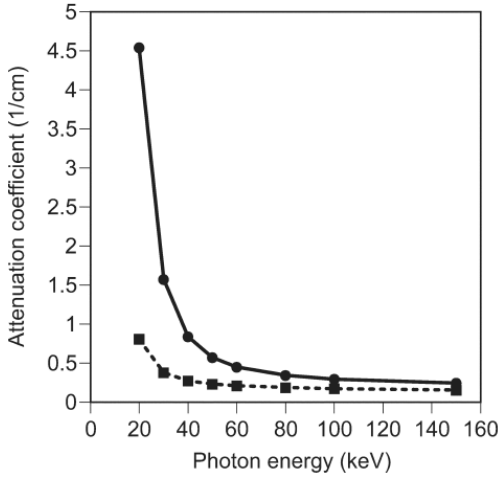

Figure 11. Attenuation coefficients of bone (solid line) and muscle (dashed line) as a function of beam energy (Copyright: Dobbins JT, Warp RJ. Dual-energy methods for tissue discrimination in chest radiography. Advances in Digital Radiography: RSNA Categorical Course in Diagnostic Radiology Physics 2003; 173-179).

The practical methods used to generate the two images at different beam energies depend on the detector technology used. It is important to understand the methods that may be used to generate images of different mean beam energy. These techniques are either one-shot or two-shot categories. The two-shot approach involves acquiring two images at different kV

settings. This method gives very good SNR properties of the resulting images because one may select the best two kV settings and best mill ampere-second values to produce the optimum subtraction. This method involves temporal delay (typically fraction of a second) between two exposures, and therefore tissues may be slightly misaligned between the two exposures due to cardiac, respiratory or gross patient movement. The one-shot approach involves only a slight x-ray exposure. Two separate detectors are placed in a sandwich configuration, such that beam hardening between the front and rear detectors change the mean detected energy of the photon beams in the two images. This technique has no temporal delay and hence no miss-registration of tissues between the low- and high-energy images[123]. The attenuation of calcifications is closer to the attenuation of soft tissue when a high-peak-kilo voltage image is obtained, whereas the attenuation of calcifications is much higher than that of soft tissues if low-energy photons are used. By adjusting the images so that the soft tissue signals match on both exposures, the soft tissue signals can be made equal, but there will still be a difference between the calcium signals. The potential method of dual-energy subtraction is difficult to achieve because of micro-calcifications are small (2-400 μm) and the two images must register perfectly in order for the subtraction to work[49, 123].

2.4.2 Contrast subtraction

Digital detectors make it possible to demonstrate the neovascularity of breast cancers with x-ray imaging[45, 109]. By using standard subtraction techniques, an image obtained before administration of contrast material (pre-contrast image) is obtained, and then subsequent images are obtained following the intravenous administration of iodinated contrast material (post-contrast images). The pre-contrast image can be subtracted from the post-contrast images, leaving only the areas containing the contrast material visible[45, 63, 109].

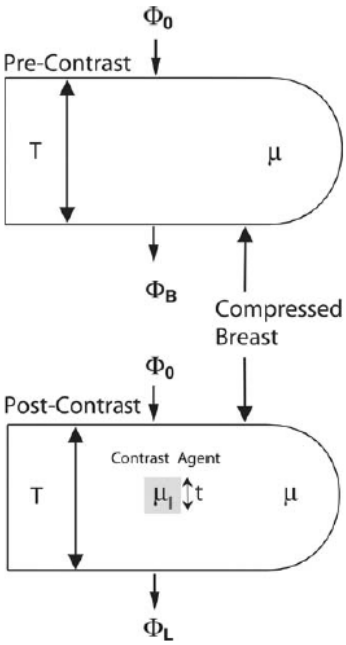

Figure 12. Schematic representation of a mask (pre-contrast) image and a post- contrast image for a simple model of digital subtraction mammography. Φ_0 is the x-ray fluency incident of the breast; Φ_B and Φ_L represent the transmitted x-ray fluencies through the breast. Before and after uptake of the iodide, T is a thickness of the breast; and t is the thickness of the lesion containing Iodide. (Copyright: Skarpathiotakis M, Yaffe MJ, Bloomquist AK, et al. Development of CDM. Med Phys 2002;29:2419-2426.

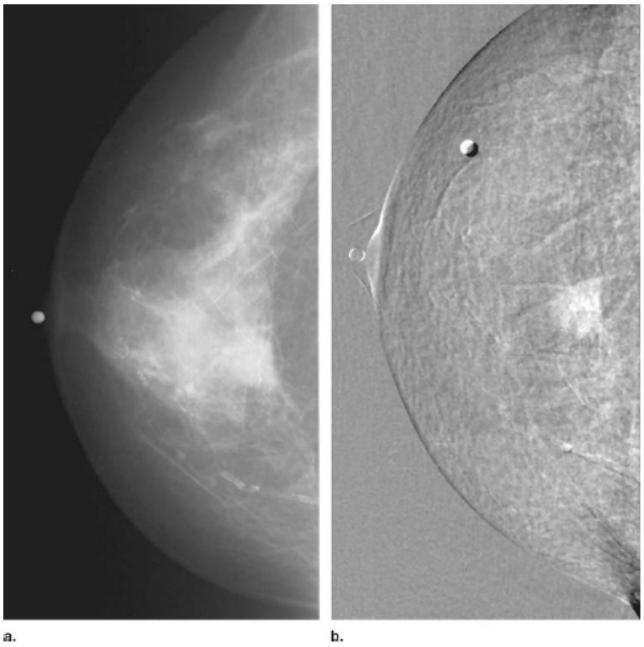

Figure 13. (a) Digitized CC SFM of patient with infiltrating lobular carcinoma and DCIS. A metallic nipple marker is seen. (b) Contrast enhanced digital mammogram subtraction CC image. Obtained 7 minutes after the start of contrast injection, shows irregular spiculated enhancement. (Copyright: Jong RA, Yaffe MJ, Skarpathiotakis M, et al. Contrast-enhanced digital mammography: initial clinical experience. Radiology 2003; 228: 842-850).

It has been shown that the growth and the metastatic potential of tumors can be directly linked to the extent of surrounding angiogenesis[134]. These new vessels proliferate in a disorganized manner and are of poor quality. This makes them leaky and permits fluid to pass out the vessels into the tumor. The use of intravenously administered contrast material takes advantage of this characteristic of tumor vessels. The use of contrast medium uptake imaging methods to aid in the detection and diagnosis of breast cancer is encouraging. Contrast-enhanced breast MRI using gadolinium based contrast agent, Gd-DTPA, has already shown to have high sensitivity and moderate specificity in the detection of breast cancer[33, 36, 37, 46, 84, 135].

2.4.3 Motivation for digital breast tomosynthesis clinical research

Traditional mammography is the single best breast cancer screening test to date and has been shown to reduce mortality from breast cancer in large randomized trials[23, 83, 118]. 2D mammography is far from perfect. Using the common definition of a missed breast cancer as a negative mammogram, screening mammography is only about 70% to 75% sensitive in current clinical practise[66, 87, 96]. At a National Cancer Institute (NCI) –sponsored workshop an expert panel reviewed all the potential breast cancer screening technologies on the horizon. They concluded that, of all technologies presented, digital mammography held the greatest promise to improve breast cancer detection[73]. Despite the expectation that digital is superior to film, many trials failed to find any difference between the two types of mammograms in terms of breast cancer detection[61, 62, 108].

The latest trial, sponsored by the NCI, part of the National Institutes of Health (NIH), was conducted by a network of researchers led by The American College of Radiology Imaging Network (ACRIN). In October 2001, at 33 different sites in the United States and Canada, the Digital Mammography Imaging Screening Trial (DMIST) enrolled 49,528 women who had no signs of breast cancer. Women in the trial received both digital and analog mammograms,

which were interpreted by two different radiologists. Breast cancer status was determined through available breast biopsy information within 15 months of study entry or through follow-up mammography ten months or later after study entry. DMIST determined that digital mammography is more sensitive in women younger than 50 years of age, women with dense breast and women within the perimenopausal and premenopausal age groups. Research found that digital mammography is the same as film for women older than 50 and for those without dense breasts. Without a change in specificity digital mammography was 14% to 27% more sensitive than film, in the three subsets of women for whom digital mammography was better[86]. Although digital mammography has already proven better sensitivity in certain subsets of women. Advanced applications, especially breast tomosynthesis will revolutionize breast cancer detection and diagnosis. It is also hoped that tomosynthesis will be able to reduce both false-negative and false-positive mammograms[60].
There is much interest and excitement in the medical community regarding this new technology. Breast tomosynthesis holds a promise of better diagnostic capabilities and cancer detection, especially increasing the specificity of breast cancer detection. Some research groups have begun to evaluate tomosynthesis in diagnostic mammography while others use tomosynthesis as a part of mammography screening.

Other tomosynthesis research areas in the future are:

- Tomosynthesis-aided needle localization and biopsy[40, 137]

  Three-dimensional location of a finding in the tomosynthesis of the breast could be determined more easily from the slice (finding is located z coordinate) and the in-plane (finding is located xy coordinates)[137].
- Contrast agent-enhanced tomosynthesis[49,137]

  Tomosynthesis might help to separate enhanced tissues that are overlapped in a two-dimensional subtraction images, allowing the morphologic structure and the volume of the enhanced lesion to be better characterized[137].
- Computer-aided detection (CAD)[40, 49,137]

  Tomosynthesis slices could be compared with 2D mammograms and because of mammographic features are better characterized with tomosynthesis, the performance of CAD may be improved[137].
- Tomosynthesis and US fusion imaging
- And other future 3D applications

  The platform of tomosynthesis offers the opportunity to directly couple other technologies such as ultrasonography, optical imaging, electrical impedance, and elastography[49].

3 OBJECTIVES OF THE STUDY

The objectives of this thesis were:

1. To investigate digital breast tomosynthesis (DBT) in diagnostic mammography by comparing digital breast tomosynthesis and screen-film mammograms or digital mammograms based on clinical performance [II and VII][*]. Study digital breast tomosynthesis as an improved clinical method to more accurately

    - Distinguish malignant lesions from benign
    - Analyze lesion margins
    - Interpret confidently the finding as a summation [I, IV, V].

2. To evaluate Tuned Aperture Computed Tomography (TACT) capability as 3D breast reconstruction algorithm in the limited angle tomosynthesis system [I, II, III, IV, V, VI, VII].

[*] Roman numerals provide reference to publication by the authors which form part of this thesis and appear at the end of this publication.

3. To demonstrate the technical and clinical performance of a real-time amorphous-selenium (*a*-Se) flat-panel detector (FPD) in full field digital breast tomosynthesis [III, VI].

4. To undertake a feasibility study combining diagnostic breast tomosynthesis and ultrasound imaging of the breast with clinical information in diagnostic mammography [IV].

5. To evaluate digital spot image quality using tomosynthesis projection images compared to screen-film and diagnostic mammography [II, VII].

4 MATERIALS AND METHODS

4.1 Patient material

The patient data included in this thesis is comprised of 250 patients. 150 patients were enrolled in Finland and 100 were enrolled in the USA. Screen-film and digital mammograms included right and left mediolateral oblique (MLO) and craniocaudal (CC) views. Diagnostic mammography (also called work-up) included lateromedial (LM) and coned-down magnification views.

4.1.1 Helsinki University Central Hospital (HUCH) Mammography Department, Helsinki, Finland

Diagnostic digital breast tomosynthesis examinations were performed on 150 asymptomatic-women. The key investigation, which was digital breast tomosynthesis (DBT) in diagnostic mammography, consisted of 60 asymptomatic-women. The potential value of digital breast tomosynthesis was investigated by testing its ability to resolve ambiguities possible lesions that were ambiguous on the screening examination. The women were selected for the study based on the fact that it was not possible to exclude the presence of breast cancer based on their screening mammography exams. Some abnormal findings seen on the images were architectural distortion, stellate look-a-like lesions, parenchymal asymmetry and density

changes. Some lesions included micro-calcifications, which were either clusters or diffusely distributed. The morphology of the micro-calcifications was casting, granular, punctate, or miscellaneous. Adjunctive diagnostic methods were core biopsy, fine needle aspiration biopsy (FNAB) or vacuum assisted biopsy. Cytological and histological results for benign and borderline findings included: fibrocystic change, tumor phylloides, cysts, fibroadenomas, fibrosis, adenosis, atypical ductal hyperplasia (ADH), ductal carcinoma in situ (DCIS) and lobular carcinoma in situ (LCIS). Results for invasive malignant findings included ductal and lobular cancers, both grades 1 and 2 were found. The pathological anatomy diagnosis (PAD) from the surgery specimens varied in the following ways: ductal, lobular, mucinous, tubulobular, multifocal tubular, invasive micropapillare cancers, fibroadenomas, adenosis, DCIS, LCIS, radial scars, tumor phylloides tumor, and papillomas. The grade of malignant tumor varied between 1 and 3.

Non-specific findings which were indications to recall the women	**N=60**
tumor-like density 6 with micro-calcifications	43
parenchymal asymmetry 0 with micro-calcifications	6
architectural distortion 3 with micro-calcifications	8
stellate (‘black star’) lesion 1 with micro-calcifications	3

Table 1. Non-specific findings: indications to recall the women at HUCH Mammography Department.

Radiological interpretation of the lesions after further work-up	**N=60**
stellate	21
circumscribed	20
architectural distortion	1
scar	1
micro-calcifications, cluster	4
no tumor	13

Table 2. Radiological interpretation of lesions after further work-up at HUCH Mammography Department.

Interventional procedures performed after breast tomosynthesis study	**N=60**
no needle biopsy	16
fine needle aspiration biopsy (FNAB)	14
core biopsy	25
vacuum assisted core biopsy	5

Table 3a. Interventional procedures performed after breast tomosynthesis study at HUCH Mammography Department.

Patients requiring surgery after breast tomosynthesis study	N=60
surgery required	26
no surgery required	34

Table 3b. Patients requiring surgery after breast tomosynthesis study at HUCH Mammography Department.

Histology results of the surgery cases	N=26
carcinoma ductal	15
carcinoma lobular	5
carcinoma micro-lobular	1
radial scar	2
fibroadenoma	1
tumor phylloides	1
adenosis sclerosans	1

Table 4. Histology results of the surgery cases at HUCH Mammography Department.

40 women were recalled for the material of combined breast tomosynthesis and ultrasound imaging, because it was not possible to exclude the presence of breast cancer on screening films. The 40 work-up recall cases were classified in categories from 1 to 4.

1 = no lesion
2 = probably benign lesion
3 = malignancy could not be excluded
4 = highly suspicious of malignancy

Abnormal findings on the screening mammograms were tumor-like densities, parenchymal asymmetries, architectural distortions, stellate lesions and micro-calcifications which were diffusely distributed or clustered. The morphology of the calcifications was punctate and were associated with architectural distortion. Focal lesions were stellate, rounded or architectural distortions. The size of the suspicious findings varied from 4 millimetres (mm) to 40 millimeters (mm). Cytological and histological results for benign lesions were: haemangioma, adenosis, fibroadenoma, fibrosis and fibrocystic change. Furthermore, results for malignant findings were ductal carcinoma in situ (DCIS) and invasive ductal cancer. The grade of malignant lesions varied between 1 and 2[121].

Abnormal screening mammogram findings	N=40
tumor-like densities	20
parenchymal asymmetries	8
architectural distortions	12

Table 5. Abnormal screening findings of 40 asymptomatic women enrolled in the study of combined breast tomosynthesis and ultrasound imaging of the breast.

Interventional procedures	N=40
no needle biopsy	16
fine needle aspiration biopsy	0
core biopsy	22
vacuum assisted biopsy	2

Table 6. Interventional procedures in the study of combined breast tomosynthesis and ultrasound imaging.

Histology of the surgical cases	N=24
ductal cancer in situ	3
ductal cancer	2
atypical ductal hyperplasia	1
fibroadenoma	2
radial scar	1
normal breast tissue	3
fibrosis	10
hemangioma	1
papilloma intraductal	1

Table 7. Histology of the surgical cases in the study of combined breast tomosynthesis and ultrasound imaging.

4.1.2. Jane Brattain Breast Center, Park Nicollet Clinic, Minneapolis, USA

The total number of women participating in the study were 100 (ages 45 to 80). All patients were recalled because additional information was needed to better determine treatment planning or because it was not possible to exclude the presence of breast cancer after screening mammography. A total of 43 invasive cancers and 3 ductal in situ carcinomas (DCIS) were detected and diagnosed. The 54 benign cases included lobular carcinoma in situ (LCIS), atypical ductal hyperplasia (ADH), fibrocystic change, fibroadenoma, cyst, scar, intracystic papilloma, hemangioma, benign microcalcifications, and summation of breast tissue, tables 8, 9a and 9b.

Indications for breast tomosynthesis study	N=100
tumor-like density	12
parenchymal asymmetry	10
architectural distortion	15
stellate (‘black star’) lesion	3
probably carcinoma	35
probably benign lesion	15
probably summation of normal breast tissue	10

Table 8. Indications for breast tomosynthesis study at Jane Brattain Breast Center.

Indications for breast tomosynthesis study, breast biopsy results	N=100
cancer	43
cancer in situ	4
atypical ductal hyperplasia	1
fibrocystic change	14
fibroadenoma	17
cyst	3
summation of the normal breast tissue	14
scar	2
intracystic papilloma	1
hemangioma	1

Table 9a. Indications for breast tomosynthesis study, breast biopsy results at Jane Brattain Breast Center.

Histology of the cancers	N=47
ductal cancer: g1 7 cases g2 19 cases g3 10 cases	36
lobular cancer: g1 1 case g2 5 cases g3 1 case	7
in situ: DCIS 3 cases LCIS 1 case	4

Table 9b. Histology of the cancers at Jane Brattain Breast Center.

4.2 Digital breast tomosynthesis systems

A small field of view digital breast tomosynthesis system, Diamond-Delta 32 TACT (Instrumentarium Imaging, now part of GE Healthcare) and the prototype of full field digital breast tomosynthesis system, Diamond DX (Instrumentarium Imaging, now part of GE Healthcare) were the two tomosynthesis systems used mainly for the research of this thesis. Diamond-Delta 32 TACT was used to investigate:

(1) Digital breast tomosynthesis (DBT) in diagnostic mammography by comparing the clinical performance of digital breast tomosynthesis images and screen-film mammograms
(2) Digital breast tomosynthesis (DBT) in diagnostic mammography by comparing the clinical performance of digital breast tomosynthesis images and full field digital mammography (FFDM).
(3) Combined breast tomosynthesis and ultrasound imaging of the breast.
(4) Digital spot image quality (=tomosynthesis projection images) compared to screen-film mammograms and diagnostic mammograms.

Diamond DX was used to demonstrate technical and clinical performance of a real-time amorphous-selenium (*a*-Se) flat-panel detector (FPD) in full field digital breast tomosynthesis. Both Diamond-Delta 32 TACT and Diamond DX were used to evaluate Tuned Aperture Computed Tomography (TACT) capability as a 3D breast reconstruction algorithm in the limited angle tomosynthesis system. The prototype of full field digital breast tomosynthesis system, Nuance (Planmeca Corporation Planmed Oy) was used to plan the research activities after this thesis. Nuance incorporates the same amorphous selenium (*a*-Se) detector as Diamond DX. This particular *a*-Se panel is developed and manufactured by Anrad Corporation, Canada. Chapter 5 introduces prototypes of full field tomosynthesis systems.

4.2.1 Small field of view tomosynthesis system

Diamond-Delta 32 TACT tomosynthesis system incorporates a charged coupled device (CCD) small-area digital detector with 48 μm pixel size. The matrix array is 1024x1024 with an active imaging area of 5 cm x 5 cm. The mammography system has generator: 20-39 kV, 2-500 mAs and 0.3 mm focal spot with a doped molybdenum dual-angle anode. We acquired seven images using stereotactic tubehead movement with the total arc of 30° (-15° to +15°) while the x-ray source moves through an arc above the stationary compressed breast and small-field of view digital detector. A reference point located in the compression paddle was used to define the imaging geometry and 3D locations were calculated based on this information. The entire breast image reconstruction time for seven projection image data sets was 50 seconds. We generated 25-50 slices and the thickness of each tomosynthesis slice was between 0.5 mm to 2.5 mm All patient images related to this study were acquired using a Mo/Mo target filter combination and without an anti-scatter grid.

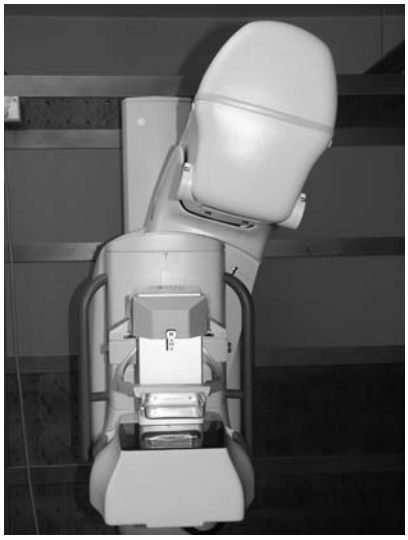

Figure 14. Small field of view digital breast tomosynthesis system, Diamond-Delta 32 TACT.

4.3 Reconstruction algorithm

A three-dimensional radiographic data-acquisition scheme called Tuned Aperture Computed Tomography (TACT) has been used in this study for 3D reconstruction[125, 126]. The method is based on optical aperture theory, which extends and completely generalizes the better-known laminographic process termed tomosynthesis[2, 30, 70, 71, 72, 76, 97, 140]. TACT is accomplished by using information associated with the irradiated object itself and/or its relationship to the image detector to determine projection geometry after the fact. This expedient permits TACT to map all incrementally obtained projection data (source images) into a single 3D matrix even when the shape of the equivalent sampling aperture is unknown. The result allows retrospective determination of purposeful changes in projection geometry required by the aiming process. The closest existing approximation is conventional fluoroscopy, which requires continuous exposure and does not allow for incremental accumulation of 3D information other than through the mental perception of depth realized from continuous interactive interpretation of dynamic 2D projections. TACT circumvents this fluoroscopic short coming by exploiting the following postulates: 1) perceptually meaningful 3D reconstructions can be produced from optical systems having any number of different aperture functions, and 2) any aperture can be approximated by summation of a finite number of appropriately distributed point apertures[127, 129]. In summary, a TACT slice can be produced from an arbitrary number of x-ray projections (each exposed from a different angle). All such projections must contain a recognizable reference point produced by a fiducially located object above the detection plane in a fixed position relative to the specimen.

A desired slice is generated by:

1) identifying the fiducially located reference point in each projected image
2) computing the center of gravity (COG) of the two-dimensional distribution of all point positions so identified
3) drawing lines between each point projection and the center of gravity
4) determining the desired slice position expressed as a fraction of the depth from actual unchanging position of the fiducially located reference point to the detector plane
5) laterally shifting each projection a distance equal to this fraction of the total distance between the image of the respective reference point and the center of gravity in a direction parallel to the line connecting the reference point and the center of gravity
6) averaging all of the resulting laterally shifted images[127, 129, 130, 131].

Using the TACT algorithm, it is possible to use one x-ray source and move it through several points in space or use several fixed sources to collect multiple x-ray projections which in turn can be processed to produce TACT slices. With this technique any number of images from various sources of source locations can yield TACT images so long as the object and image plane relationship do not change. In any case, the ‘thickness’ of the image layer is determined solely by the degree of angular disparity between the most extreme source locations. This is analogous to the wider aperture of a camera lens producing a thinner image plane. The ‘thickness’ of the image layer can be adjusted or tuned to the diagnostic task by increasing or decreasing the angular disparity between the sources or single-source positions[129].

The total absorbed dose to the patient required for TACT need not substantially exceed that required by a single projection of comparable signal-to-noise ratio produced from a detector having the same quantum efficiency. One way of interpreting this relationship is to consider a TACT image as being the algebraic sum of a set of N nearly identical projections, each of them produced from approximately 1/N of the dose of a single transmission 2D projection. To the extent that each image is identical, only the quantum mottle varies from one to the next. Summing the images is equivalent to averaging the quantum variations so that the resulting image has the same quantum statistics as an image produced by an ideal detector using a single exposure N-times as long[127].

All linearly derived tomographic TACT image displays significantly increased the detectability of simulated mammographic details relative to the conventional transmission-based mammography. This observation is remarkable because of TACT's relative independence from all other significant interactive effects (main effects, modality, density, exposure, observer, task, significant 2-way interactions, density and mode, density and task, exposure and task, modality and task, observer and task, significant 3-way interaction, sensity, modality and task)[131].

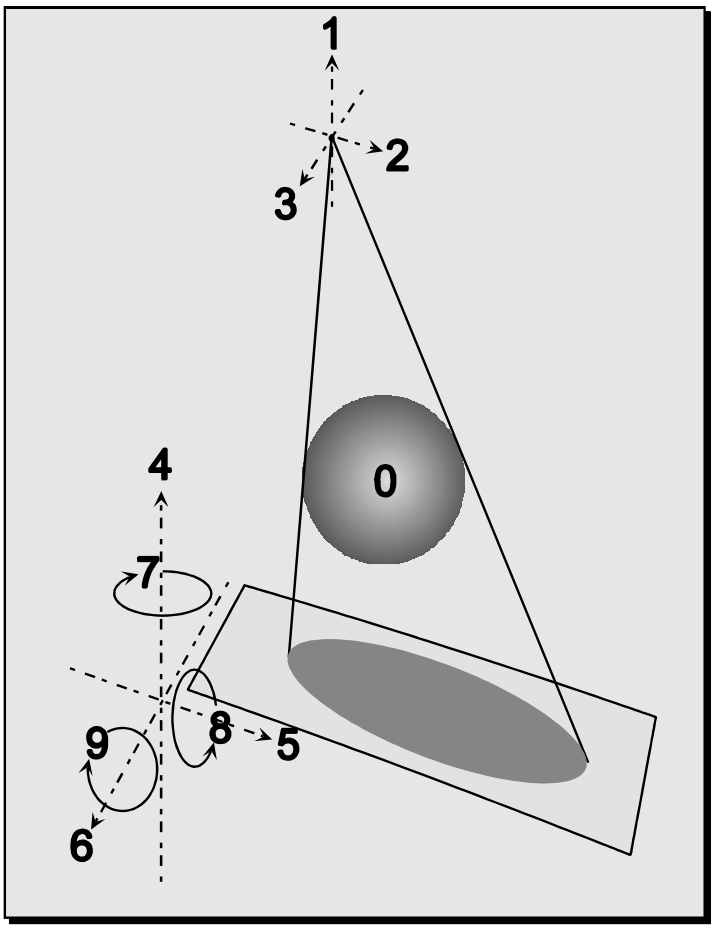

Figure 15. TACT required information; a projection based 3D imaging method (Copyright Dr Richard Webber).

4.4 Data analysis and statistical methods

4.4.1 Clinical tomosynthesis images

Asymptomatic women enrolled in the study based on prior identification of suspicious findings on screening mammograms where the possibility of breast cancer could not be excluded. Two or three experienced radiologists in screening and diagnostic mammography independently reviewed screening, diagnostic mammograms and digital breast tomosynthesis studies performed on the same patients. Screening mammograms were taken either with screen-film or digital mammography systems. Mammography work-up examination (film imaging) included lateromedial and coned down magnification views. Adjunctive diagnostic methods used (if needed) included additional views, ultrasound, FNAB, and core or vacuum assisted biopsy.

The Likert scale used in this study was as follows:

-4 two-dimensional mammography images are absolutely better
-3 two-dimensional mammography images are clearly better
-2 two-dimensional mammography images are better
-1 two-dimensional mammography images are a little better
0 two-dimensional mammography images and tomosynthesis images are equal
+1 tomosynthesis images are a little better
+2 tomosynthesis images are to some extent better
+3 tomosynthesis images are clearly better
+4 tomosynthesis images are absolutely better

The evaluation was made under six conditions at Helsinki University Central Hospital:

tomosynthesis slice images versus screen-film mammograms
tomosynthesis slice images versus diagnostic film mammograms
tomosynthesis volume model versus screen-film mammograms
tomosynthesis volume model versus diagnostic film mammograms
tomosynthesis two-dimensional projection images versus screen-film mammograms
tomosynthesis two-dimensional projection images versus diagnostic film mammograms

The evaluation was made under two conditions at Jane Brattain Breast Center:

tomosynthesis slice images versus screening FFDM images
tomosynthesis volume model versus screening FFDM images

In Chapter Appendix (page 62) Digital Breast Tomosynthesis (DBT) evaluation form is presented.

4.4.2 Statistical analysis

Statistical analysis used in this thesis was the *t* test. The *t* test assesses whether the means of two groups are statistically different from each other. This analysis is appropriate whenever you want to compare the means of two groups, and specially appropriate as the analysis for the post-test-only two-group randomized experimental design. Figure 16 shows the distributions for the treated and control groups in a study. The figure shows idealized distribution, the actual distribution is usually depicted with a histogram or bar graph. It indicates where the control and treatment group means are located. The question the *t* test addresses is whether the means are statistically different. What does it mean to say that the averages for two groups are statistically different? Consider the three situations: A case with moderate variability of scores within each group, the high variability case and the case with low variability. The formula for the *t* test is a ratio. The top part of the ratio is the difference between the two means or averages. The bottom part is a measure of the variability or dispersion of the scores. This formula is essential to another example: the signal-to-noise metaphor in research: the difference between the means is the signal that, the bottom part of the formula is a measure of variability that is essentially noise that may make it harder to see the group difference. The top part of the formula is easy to compute by finding the difference between the means. The bottom part is called the standard error of the difference. To compute, take the variance for each group and divide it by the number of people in that group. Add these two values and take their square root. The specific formula is:

$$SE(\bar{X}_T - \bar{X}_C) = \sqrt{\frac{var_T}{n_T} + \frac{var_C}{n_C}}$$

The variance is the square of the standard deviation. The final formula for the *t* test is:

$$t = \frac{\bar{X}_T - \bar{X}_C}{\sqrt{\frac{var_T}{n_T} + \frac{var_C}{n_C}}}$$

The *t* value will be positive if the first means is larger than the second and negative if it is smaller. Once you compute the *t* value, look it up in a table of significance to test whether the ratio is large enough to say that the difference between the groups is not likely to have been a chance finding. To test the significance, one must set a risk level, called the alpha level. In most social research the rule of means is to set the alpha level at .05. Five times out of a hundred a statistically significant difference would be found between the means even if there was none. The degrees of freedom for the test must be determined. In the *t* test, the degrees of freedom is the sum of the persons in both groups minus 2. Given the alpha value, the degrees of freedom, and the *t* value, one would be able to look the *t* value up in a standard table of significance to determine whether the t-value is large enough to be significant. If it is, it can

be concluded that the difference between the means for the two groups is different (even given the variability)[18, 27, 32, 38, 69, 77].

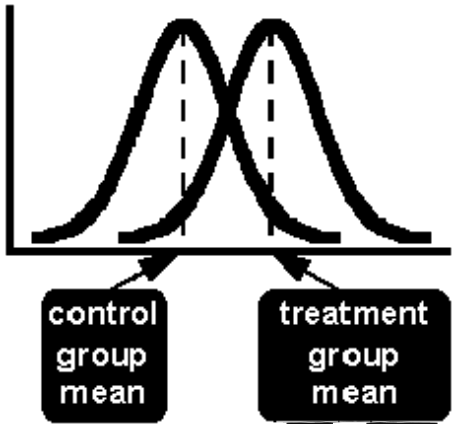

Figure 16. Idealized distributions for treated and comparison group posttest values

5 TECHNICAL CHARACTERIZATION OF FULL FIELD TOMOSYNTHESIS SYSTEM

5.1 Full field of view tomosynthesis system

The prototype for full field digital breast tomosynthesis system Diamond DX incorporates amorphous selenium (*a*-Se). The effective flat-panel detector (FPD) area consists of 2816 x 2016 pixel matrix having a pixel pitch of 85 μm. This yields to a theoretical maximum spatial frequency of 5.9 lines per mm. The biasing voltage of 2 kV is applied over 200 μm thick *a*-Se layer. Flat field correction is applied on 13bit raw is to eliminate the differences in pixel responses and to correct possible defects[53, 57, 67, 68, 88, 120]. The prototype of tomosynthesis full field digital mammography system used is based on real-time *a*-Se FPD technology. The main advantage of this particular detector is that it is derived from the same technology employed in a fluoroscopic detector[119]. The selenium layer used in the real-time detector uses unipolar-conducting blocking layers to create a p-i-n structure, which allows charged images to reach their corresponding collection electrodes, and prevents the injection of leakage charge from the collection electrodes into the selenium. This unique structure allows rapid readout of the array since the only limiting factors that affect lag and ghost are material imperfections. Two modes of operation are defined for this detector, one for conventional screening exams, and one for tomosynthesis exams.

Figure 17. The prototypes of full field digital breast tomosynthesis system, Diamond DX and Nuance based on *a*-Se FPD technology.

5.1.1 Screening and tomosynthesis mode

There are two primary differences between the modes of operation, namely the frame rate and the dynamic range. For the screening exam, the read time for the detector is 1.3 seconds with a fixed integration period of 2.8 seconds. This provides a frame rate of one frame for every 4.1 seconds. Tomosynthesis imaging requires several images of the breast to be acquired as quickly as possible. For this mode the detector read time would be decreased to 400 ms, and the integration time set to 100 msec. This gives a frame rate of one image every 500 ms. The dynamic range for screening mode is better than 1200:1. Since multiple images are required for the tomosynthesis mode, the offset map cannot be updated between exposures in this mode and therefore must be updated before the procedure begins. The gain of the amplifier stage of the detector is increased to reduce the effect of electronic noise, since the exposure per frame is much lower for tomosynthesis imaging than in screening exams. This increased gain of the preamplifiers reduces the overall dynamic range of the detector to about 800:1[82]. The 2816 x 2016 array is connected to custom readout ASIC's and commercially available scan drivers through tape-automated bonding (TAB) technology. The total arc of the breast tomosynthesis system is 30°-40° and tomosynthesis sequence of 15 low-dose exposures is performed at approximately 1-1.5 times the radiation dose of a conventional mammogram.

5.1.2 Image ghosting

The concerns of image ghosting when performing breast tomosynthesis with a large 3584 x 2816 detector array have been studied in the screening mode by using a similar technique. The ghosting was measured by delivering a small read dose on several frames, delivering the ghost exposure, and then measuring the sensitivity by delivering the same small read dose after the ghost. The read dose was defined by 28 kVp Mo/Mo filtered by 4 cm PMMA, and

an exposure of 50 mAs, which corresponds to a detector entrance dose of 5.5 mR. No change in detector response could be seen after the ghost on either detector compared to the initial response prior to the ghost image. To be able to visually demonstrate the ghosting performance, a typical screening exam was simulated using an ACR accreditation phantom. The phantom was placed on the surface of the detector and imaged with 26 kVp, 100 mAs exposure, which translates to an exposure of 1100 mR to the detector, and an exposure to the detector underneath the phantom of around 33 mR (including scatter). Thirty seconds later, the phantom was moved to a new location, which partially overlapped the previous position, and re-imaged with the same technique. Since there is a large difference in exposures between the open field and underneath, the edge of the ACR phantom represents a very high contrast object which can render a ghost. Since the ACR phantom is a radiographically uniform attenuator, any ghost artifact would be easily visible in that image. The process was repeated 4 times to emulate the four views acquired in a screening exam, and the images were reviewed to see if there were any residual ghosting artifacts. No ghosting artifacts could be seen in any of the four images[67, 68].

5.2 Physical measurements of full field digital breast tomosyntesis system

Diamond DX was used to demonstrate technical and clinical performance of a real-time amorphous-selenium (*a*-Se) flat-panel detector (FPD) in full field digital breast tomosynthesis. The performance of a digital detector can be described in terms of a number of performance factors: modulation transfer function (MTF), noise power spectrum (NPS), detective quantum efficiency (DQE). Among them, sharpness and noise are two key characteristics that describe the intrinsic image quality performance[99]. Results are presented in Chapter 7.

5.2.1 Modulation transfer function (MTF)

The MTF is a plot of the ratio of the output-to-input modulations as a function of spatial frequency. The higher the MTF, the better the sharpness and resolution of an image. There are two advantages of using the MTF to describe the sharpness properties of an imaging system. First, the sharpness can be characterized at multiple levels of detail (spatial frequencies). Second, if a system has multiple components, each of which affects its sharpness, the MTF of the overall system, under suitable conditions, is simply a multiplication of the MTFs of the individual component. Mathematically the MTF is the Fourier amplitude of the point spread function (PSF)[99].
The resolution of the digital detector was measured using a 10 μm wide slit (Nuclear Associates 07-624-1000), placed at small angle with respect to the vertical detector element lines, directly on the detector. Images of the slit were acquired using a 28 kVp Mo/Mo spectrum with an exposure of 16 mAs. A composite line spread function (LSF) was then calculated by oversampling the slit image using the technique described in the literature[9, 25]. The corresponding MTF was then calculated by taking the discrete Fourier transform of the LSF[68].

5.2.2 Noise power spectrum (NPS)

Noise refers to 'unwanted' image details that interfere with the visualization of an abnormality of intrest and with the interpretation of an image. This image details fall into two categories, anatomic and radiographic noise. The noise power spectrum (NPS) is the variance of noise within image divided among various spatial frequency components of the image. Mathematically, the NPS is the normalized squares of Fourier amplitudes averaged over an ensemble of noisy but otherwise uniform images[99].
7 different images were calculated to remove any low level fixed pattern noise effects. This approach is valid since the relative spatial gain variation is rather small from pixel to pixel. From each different image, two 256 x 256 NPS estimates (2x7 difference images) were then averaged together to obtain a 2D NPS. With the exception of on-axis components, the NPS are essentially isotropic in nature. Therefore, 1D NPS were extracted from the 2D NPS data sets be taking 8 lines above and below the f_x=0 horizontal x-axis, and re-binning the data to account for slight variations in the spatial frequency. Finally the MTF and NPS data were used to calculate the DQE[68].

5.2.3 Detective quantum efficiency (DQE)

A single metric commonly used to characterize the performance of the imaging system is known as detective quantum efficiency (DQE). The DQE of an ideal system is equal to unity at all frequencies. Because SNR^2 (actual) is always less than SNR^2 (ideal), the value of the DQE is always less than 1. The higher DQE, the better are the SNR characterization[99].
DQE of this system was measured by acquiring 8 flat field images for each exposure level of interest. To demonstrate the performance of the detector for tomosynthesis application, the detector gain was adjusted to reflect the timing sequence. The spectrum for these measurements was from a 28 kVp Mo/Mo beam filtered by 30 µm Mo and 4 cm PMMA. The PMMA was attached to the head of the collimator to minimize the impact of scattered radiation on the measurement. The measured HVL for this spectra was 0.591 mm aluminium. From this measurement, and the tables published by Boone[6], the photon fluence was estimated to be 4.9 x 10^4 photons/mR/mm^2. In this measurement, the corresponding exposure was measured with a Keithley model 35050A dosimeter. From the 8 flat field images, a ROI of 256 x 512 was extracted from each image near the center of the array. From each of the 8 ROI's, 7 difference images were calculated to remove any low level fixed pattern noise effects[68].

5.2.4 The ghost of the selenium detector

All FPDs, using both direct and indirect conversion technologies, had various degrees of temporal artifacts which lead to ghost images[54, 85, 107]. The origin of these ghost images has some similarities and differences between technologies. In indirect conversion detectors, ghost images can arise from (i) phosphor afterglow, (ii) charge trapping in the *a*-Si:H photodiode, (iii) charge trapping in the *a*-Si:H TFT, and (iv) incomplete readout of the pixel. For direct conversion detectors, the origins of ghost are (i) leakage current through the direct conversion material, (ii) charge trapping in the direct converter material structure, (iii)

trapping in the *a*-Se:H TFT, and (iv) incomplete readout of the pixel. For most applications offset ghost mechanisms can be easily compensated for since there is adequate time between exposures to measure the offset of the detector dynamically, and subtract it from the actual x-ray image to minimize the ghost. For real-time applications such as tomosynthesis, it is more difficult to dynamically update the offset since every frame is exposed with x-rays. The raw lag of the detector is an important factor to consider for these advanced applications. For direct conversion static detectors, it has been shown that these with a reset scheme between frames can be used to minimize the sensitivity of the ghost. The raw offset and sensitivity of the ghost of the selenium detector were measured. Several dark frames were acquired, followed by a single frame exposure of x-rays. The total exposure delivered during this ghost exposure was varied between 37 mR and 111 mR to simulate exposure conditions envisioned near the periphery of the breast tomosynthesis application. The data was normalized to the response of the x-ray frame to provide a measure of lag in percent. Ghost performance due to gain variations were also investigated. Several frames were acquired with relatively low exposure levels (3.7 mR), followed by two frames of high exposure (83 mR). Subsequent frames were then acquired back at the low exposure gain[68].

5.3 Additional mastectomy breast phantom

A special mastectomy breast phantom made by Peter B. Dean, MD was utilized in the technical and clinical performance evaluation of a real-time amorphous-selenium (*a*-Se) flat panel detector (FPD) in full field digital breast tomosynthesis. The phantom was composed of mastectomy specimen (Figure 18) and had a thickness of 5.0 cm[57]. The other phantom used was a contrast detail phantom (RMI 180) embedded in turkey breast tissue. Superimposed on the breast tissue were synthetic fibres to create high frequency objects to simulate vascular structures of real breast tissue. The overall thickness of this phantom was about 6.0cm.

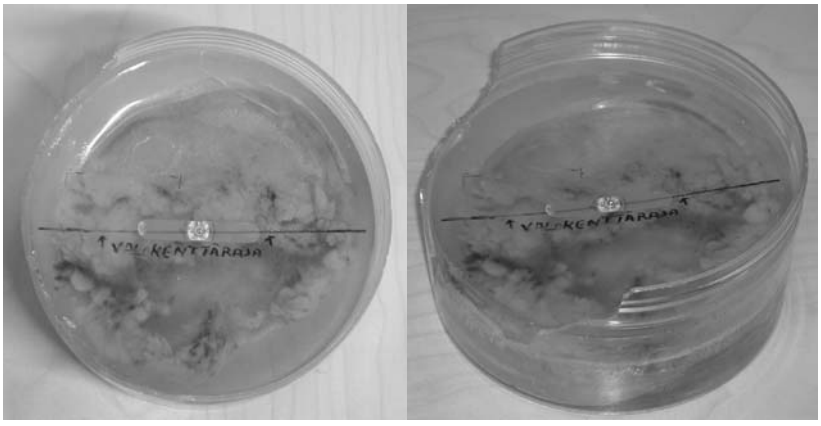

Figure 18. Mastectomy breast phantom used in full field digital tomosynthesis system evaluation.

5.3.1 Breast tomosynthesis phantom studies

Two breast phantom tomosynthesis studies were also performed to compare qualitative tomosynthesis image quality with 2D images. The first study was as follows: projection

images were acquired at 28 kVp, 20 mAs, Mo/Mo anode filter combination without a grid. Average glandular dose (AGD) per projection image was 0.33 mGy. The total arc was 30º as the x-ray source moves above the stationary compressed breast phantom and FPD. TACT reconstruction method was used for reconstruction[57].

The second study was performed with a phantom consisting of a contrast detail phantom (RMI 180) embedded in turkey breast tissue. A 2D image was acquired using an exposure of 28 kVp and 125 mAs. For tomosynthesis projection images, 9 low dose images were acquired at 28 kVp and 28 mAs, with the total arc of 20º. TACT reconstruction algorithm was used[68].

6 CLINICAL RESULTS

6.1 Digital breast tomosynthesis (DBT) in diagnostic mammography by comparing digital breast tomosynthesis and screen-film and digital mammograms clinical performance

Clinical image quality was evaluated independently by three experienced radiologists using the Likert scale explained earlier in Chapter 4. The statistical method used was *t* test. Digital breast tomosynthesis slices and volume model were compared with screen-film mammography (SFM) and diagnostic film mammography (DFM) images. The result of the *t* test shown in table 10 indicates that the clinical image quality is better in breast tomosynthesis slices than in SFM and DFM. When analyzing screening findings, tomosynthesis aids the radiologists by increasing specificity. The tomosynthesis volume model should be used as a supporting tool for tomosynthesis slices. Therefore diagnosis should not be made from only a tomosynthesis volume model like in CT and MRI. Although SFM and DFM results are unable to demonstrate that those would be better than tomosynthesis volume model. Table 11 illustrates the results in the paired *t* test, showing a significant difference in results between radiologists [II and VII].

(N=180)	*t* value	Std. Error	*t* test; ($P < 0.001$)
tomosynthesis slice images versus screen-film mammography (SFM) images	1.23	0.15	accept
tomosynthesis slice images versus diagnostic film mammography (DFM) images	0.82	0.15	accept
tomosynthesis volume model versus SFM images	-0.11	0.15	reject
tomosynthesis volume model versus DFM images	-0.40	0.15	reject

Table 10. *t* test results.

Radiologist 1 versus radiologist 2	0.06
Radiologist 1 versus radiologist 3	0.82
Radiologist 2 versus radiologist 3	0.11

Table 11. Values from the paired *t* test.

6.2 Tuned Aperture Computed Tomography (TACT) capability as 3D breast reconstruction algorithm in the limited angle tomosynthesis system

Based on all results presented in this thesis, TACT algorithm is used and capability as 3D breast reconstruction algorithm is proven in a limited angle tomosynthesis systems. Utilizing a reference point in the compression paddle to define the imaging geometry, coupled with very fast reconstruction time are two major advantages for TACT. 3D locations of the breast were calculated based on this information. The tomosynthesis system was not sensitive to mechanical movements or exact angle information given TACT's flexibility. Reconstruction time for a 10 image data set was approximately 45 seconds. [I, II, V and VII].

6.3 Digital breast tomosynthesis as an improved clinical method with greater potential to distinguish possible malignant from benign, analyze lesion margins and interpret confidently the findings as a summation

The comparison of digital breast tomosynthesis slice images versus screening FFDM images and tomosynthesis volume model versus screening FFDM images were evaluated by three experienced radiologists. The Likert scale explained in chapter 4 was used with results presented in two tables. Table 12 summarizes the benefits of benign cases and table 13 explains the benefits of malignant cases. Digital breast tomosynthesis was found to be an improved method by providing greater opportunity to distinguish possible malignant from benign, analyze lesion margins and interpret confidently the finding as a summation [I, IV and V]

Indication for digital breast tomosynthesis (DBT) clinical benefit	**Number of cases where DBT was better (N=53)**	**Diagnostic benefit of tomosynthesis by increasing specificity**
Probably benign lesion; analyze the lesion margins	20	38% (20/53 cases)
Summation of the breast tissue	14	26% (14/53 cases)
Number of unnecessary biopsies	36	68% (36/53 cases)
Analyze the finding; abnormality is present or not	40	75% (40/53 cases)
Reduce number of follow-up exams	30	57% (30/53 cases)

Table 12. Digital breast tomosynthesis (DBT)
An improved clinical method studying the following benign cases.

Indication for digital breast tomosynthesis (DBT) clinical benefit	**Number of cases where DBT was better (N=47)**	**Diagnostic benefit of tomosynthesis by increasing specificity**
Analyze tumor margins	30	64% (30/47 cases)
Multifocality, multicentricity	10	21% (10/47 cases)
Detection of small non-palpable breast cancers	3	6% (3/47 cases)

Table 13. Digital breast tomosynthesis (DBT)
An improved clinical method studying the following malignant cases.

6.4 Digital spot image quality (= tomosynthesis projection images) compared to screen-film and diagnostic mammography

Tomosynthesis projection images were compared in contrast to screen-film mammography and diagnostic film images by three experienced radiologists. Table 14 summarizes the result of the *t* test. Results indicate that tomosynthesis projection images provide diagnostic value and benefits over SFM and DFM images. DFM could be replaced by tomosynthesis projection images which are the data for tomosynthesis 3D reconstruction [II and VII].

(N=180)	***t* value**	**Std. Error**	***t* test; ($P < 0.001$)**
tomosynthesis two-dimensional projection images versus SFM images	1.18	0.15	accept
tomosynthesis two-dimensional projection images versus DFM images	0.64	0.15	accept

Table 14. *t* test results.

6.5 Combining diagnostic breast tomosynthesis and ultrasound imaging of the breast clinical information in diagnostic mammography

Forty women were recalled for further workup because it was not possible to rule out the presence of breast cancer on their screening films alone. The 40 work-up cases were classified in categories from 1 to 4:

1 = no lesion,
2 = probably benign lesion,
3 = malignancy could not be excluded
4 = highly suspicious of malignancy

After completion of the mammography work-up examination, if a specific radiological diagnosis was still missing, a breast tomosynthesis study was performed. Ultrasound alone did not show any lesions clearly, but we were able to analyze and locate the lesions exactly when using tomosynthesis and ultrasound together. Diagnostic breast tomosynthesis helped radiologists to analyze screening findings by increasing radiological specificity, and target verification was more accurate. Color Doppler information from ultrasound and diagnostic breast tomosynthesis is a combined imaging method allowing enhanced study of difficult cases while providing a specific diagnosis [IV].

Clinical benefit	**Number of the cases where DBT was better (N=40)**	**Diagnostic benefit of tomosynthesis and ultrasound by increasing specificity**
Number of decreased biopsies	16	40% (16/40 cases)
Analyze the finding; abnormality is or is not present	14	35% (14/40 cases)
Summation of the normal breast tissue	8	20% (8/40 cases)

Table 15. Study results: combined breast tomosynthesis and ultrasound imaging of the breast. Images were interpreted by two radiologists.

7 TECHNICAL PERFORMANCE OF FULL FIELD TOMOSYNTHESIS SYSTEM

7.1 Technical performance of a real-time amorphous-selenium (*a*-Se) flat-panel detector (FPD) in full field digital breast tomosynthesis

The MTF is a measure of the ability of an imaging detector to reproduce image contrast at various spatial frequencies. The higher the MTF, the better the sharpness and resolution of an image[99].

Figure 19 shows the (a) measured LSF and (b) corresponding MTF characteristics of the selenium detector. At the Nyquist frequency of 5.9 lp/mm; a modulation of more than 43% is measured, which demonstrates improved resolution performance over indirect detector technologies.

The advantage of slit method, which was used, includes: (a) high precision and (b) the acceptance of the method as an established method to measure the MTF. The disadvantage includes the need for precise alignment of the slit device, which makes the measurement sometimes time-consuming. The method suffers from noise in the tails of the line spread function, necessitating the use of high or multiple exposures and the extrapolation of the tails of the LSF which imposes an a priori function and reduces the precision of the low-frequency component of the MTF[99] [III and VI].

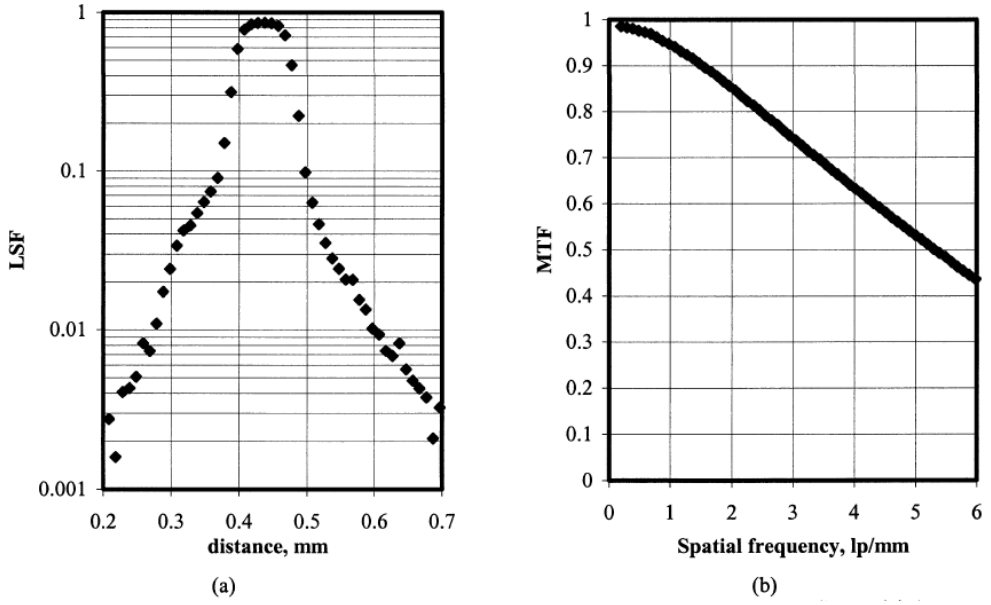

Figure 19. (a) Over sampled line spread function measured with a 10 μm wide slit (b) Corresponding modulation transfer function.

Radiographic noise is often used to describe two quantities, absolute and relative noise. The absolute noise refers to the absolute magnitude of fluctuations within the image (pixel standard deviation), while the relative noise refers to the magnitude of image fluctuations relative to the signal present in the image (pixel standard deviation divided by mean pixel). The lower the NPS, the better or lower the noise within the image. A highly uncorrelated noise pattern will render a sharply peaked autocorrelation function and a broad NPS. A Correlated noise pattern will have a broader autocorrelation function and a narrower NPS. Because radiographic noise noise does not include anatomic variations, the appropriate image for either definition is a uniform flat field exposure with no object in the field of view[99].
Figure 20(a) shows some of the 2D NPS for different entrance exposures. Figure 20(b) shows 1D NPS data extracted for calculating the DQE measurements. The magnitude of the of the noise within a radiographic image is proportional to the number of quanta used to the form of image [III and VI].

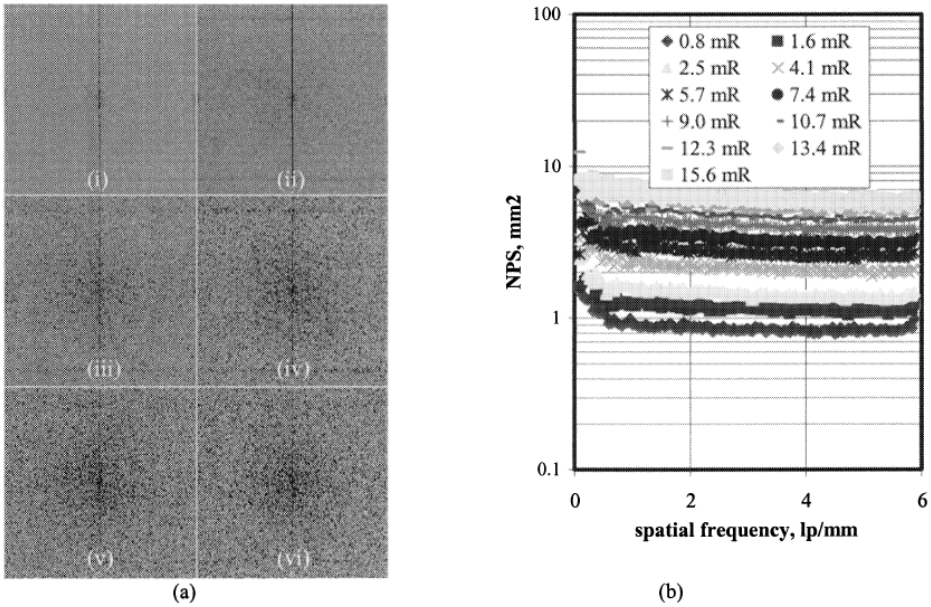

Figure 20. (a) 2D noise power spectra for (i) 0.8 mR, (ii) 2.5 mR, (iii) 5,6 mR, (iv) 9.0 mR, (v) 12.3 mR, and (vi) 15.6 mR. (b) Corresponding 1D NPS spectra extracted form 2D data sets.

The DQE provides an exposure independent measure of detector performance in the absence of non-quantum sources of noise[99].
Figure 21 shows the DQE measurement results [III and VI].

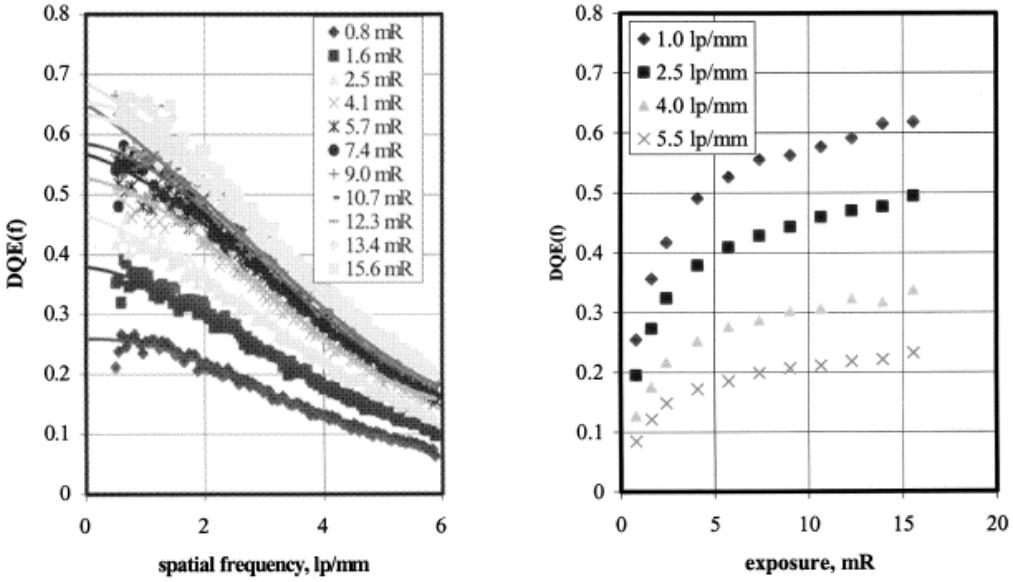

Figure 21. (a) Frequency dependent DQE acquired over exposure range from 0.8 mR to 15.6 mR. (b) Data plotted as a function of exposure for various spatial frequencies.

The lag artifacts are the form of residual signals from previous acquisitions that appear in subsequent images.
As shown in figure 22, the lag drops to about 0.4% after 3 frames. Figure 22(b) almost no change in signal level is observed due to the presence of the high dose exposure [III and VI].

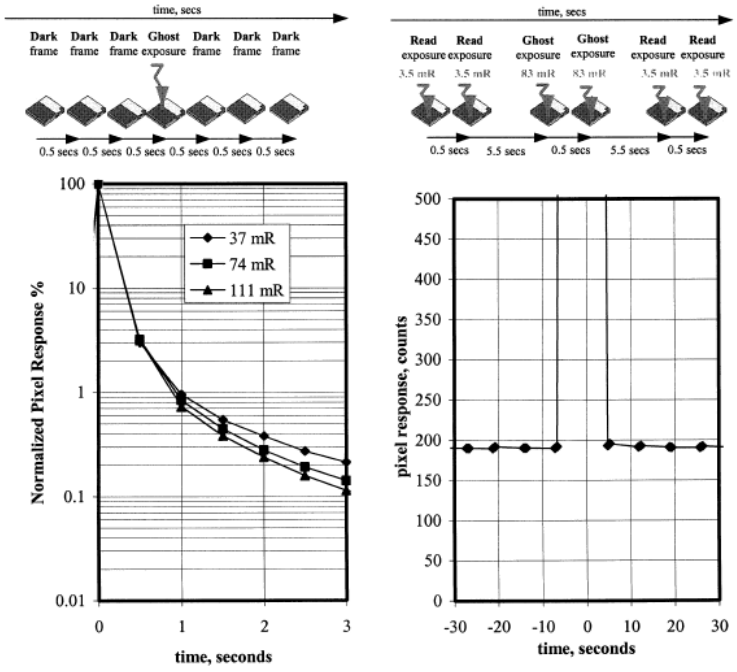

Figure 22. (a) Measurement technique and results of lag measurements
(b) Measurement technique and results of ghosting measurements on the selenium flat-panel detector.

7.2 Clinical performance of a real-time amorphous-selenium (a-Se) flat-panel detector (FPD) in full field digital breast tomosynthesis

Two breast phantom tomosynthesis studies were also performed to compare qualitative tomosynthesis image quality with 2D images. First, the phantom consisted of a contrast detail phantom (RMI 180) embedded in turkey breast tissue. Superimposed onto the breast tissue were synthetic fibers to create high frequency objects to simulate vascular structure found in real breast tissue. The overall thickness of this phantom was about 6cm. A 2D image was acquired using an exposure of 28 kVp and 125 mAs. Nine low dose tomosynthesis images were acquired using 28 kVp at 28 mAs, with a total arc of 20º. The TACT algorithm was then applied for reconstruction. Figure 22 shows the high dose 2D image, where targets found in the contrast detail phantom were extracted from the tomosynthesis data set. Figure 23 shows the extracted tomosynthesis slice in which the contrast detail targets are much more clearly visualized. Second, a special mastectomy phantom was used, shown in figure 24. This study demonstrates the capability to view the imaging plane without obscuration by surrounding structures [III and VI].

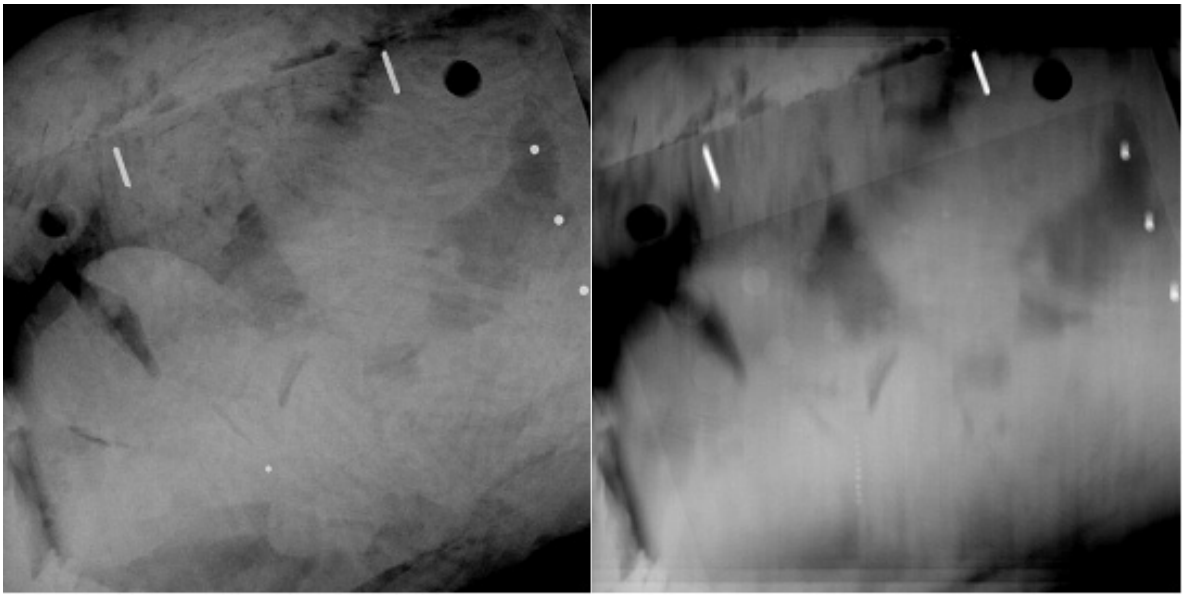

Figure 23. The phantom itself consists of a contrast detail phantom (RMI 180) embedded into the turkey breast tissue. (Left image) Normal 2D image of the phantom with 28kVp 125mAs, where the contrast details are difficult to visualize due to the overlapping structures. (Right image) Reconstructed tomosynthesis slice, where the contrast details are much more clearly visualized due to the fact that the tissue outside the plane of interest is partially blurred by the reconstruction algorithm.

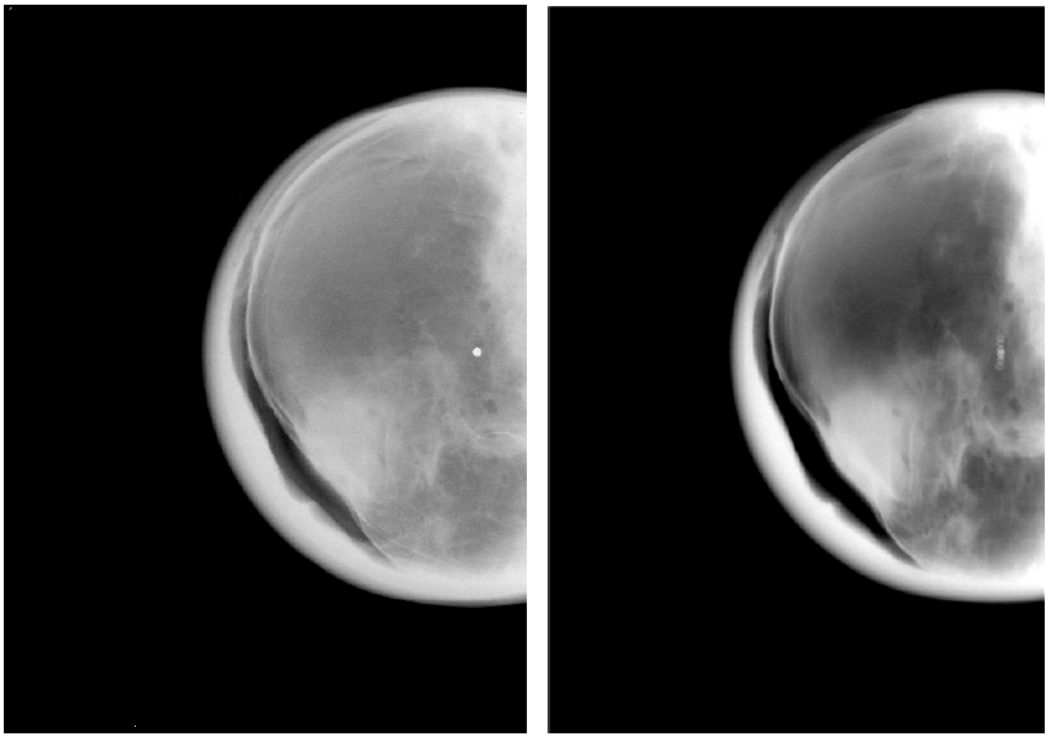

Figure 24. Example of 2D projection image (left) and tomosynthesis slice image (right) taken at 28kVp 20mAs.

8 DISCUSSION AND CONCLUSION

A variety of risk factors for breast cancer have been identified, including genetic, hormonal, morphologic, radiation-linked, nutritional, and others. In particular, additional risk factors included were a patient's personal history of breast cancer, a history of pre-menopausal breast cancer in a patient's mother and/or sisters, and a previous biopsy finding of proliferative breast disease with atypia[16]. A large number of women will develop breast cancer during their lifetime. However, in over 75% of women with breast cancer, none of these factors are present; the only clearly identifiable risks are gender and aging[4]. Many, if not most of these women, could be cured if the cancer was detected when it was quite small and still confined to the breast. Discovery of a breast cancer in its most early stage requires optimum methods in breast cancer detection. The ability to make the breast cancer diagnosis early is dependent on proper equipment, meticulous attention to technical consideration, familiarity with recognition of early and indirect mammographic signs of malignancy, and correlation with clinical signs and symptons[74]. Often breast cancer is more readily detected in the older patient population and those patients with fatty breast tissue[75], while mammograms of extremely dense tissue are more challenging to interpret.

8.1 Breast tomosynthesis

Breast tomosynthesis has the potential to detect breast cancers earlier and the ability to discover very small cancers in very dense tissue. The goal is to detect, differentiate and diagnose breast cancer before it becomes symptomatic. Most breast cancers are still found by the patient (symptomatic) and not by means of screening (asymptomatic). In screening mammography radiologists compare yearly exams, looking for subtle changes in the breast, in an effort to discover early any unsuspected disease in apparently healthy persons. A great deal has been learned from the randomized trials of breast cancer screening. The adverse effects of screening (recall of nonmalignant cases vs. over diagnosis) provides an acceptable balance, although further improvements remain a target for future research and audit[15, 21, 31 , 42, 116, 117]. The analysis of digital breast tomosynthesis have shown the following clinical benefits: improvement of overall lesion detection and analysis, increase accuracy to either confirm or exclude a suspected abnormality and in particular, detection capability of small breast cancers. The results indicate that breast tomosynthesis has the potential to significantly advance diagnostic mammography, as well as in screening mammography in the future. Based on the clinical study, tomosynthesis of the breast will increase specificity. This will lead that tomosynthesis is capable finding more cancers at an earlier stage and a smaller size than is possible in 2D mammography. Digital breast tomosynthesis is a new breast imaging modality which has proved to have advantages over 2D mammography. Breast tomosynthesis will lead to the earlier breast cancer detection and diagnosis and will keep the false positive rate as low as possible[55, 56, 57, 58, 121].

8.2 Small breast cancer detection and diagnosis

With the current increased use of mammography screening, it has become more and more important that radiologists have the ability to recognize the earliest presenting features of carcinomas. Some non-palpable cancers demonstrate conventional mammographic features of malignancy, albeit on a smaller than usual scale, whereas others present with mammographic signs that are far from characteristic of malignancy. The most difficult of early cancers to detect by mammography are those that contain no micro-calcifications and are also obscured by isodense fibroglandular tissue, impairing visualization of the cancer's central mass. For cases of unexplained focal architectural distortion, many times several benign lesions must be biopsied to insure removal of each cancer. A very minute cancer may demonstrate mammographic features so subtle that it exhibits neither poorly defined mass nor focal architectural distortion. The only clue to its existence may be the interval appearance on mammograms of a small focus of increased density[50, 98, 104, 105, 106, 125, 126]. Success in mammography screening and diagnostic mammography requires not only full knowledge of the subtle features with which very small cancers can present, but also the best methods and equipments. Mammographic detection of non-palpable breast cancer permits earlier diagnosis, more treatment options with better patient outcomes, and reduces mortality from the disease. The increasing emphasis on breast screening asymptomatic women with mammography is escalating the responsibility for earlier tumor detection more and more[121].
A non-palpable yet suspicious lesion seen on only one of the two standard projections with conventional 2D mammography may clearly be demonstrated or excluded with breast

tomosynthesis imaging. Breast tomosynthesis can prove immensely valuable when conventional mammography shows barely perceptible or extremely subtle findings that are too innocuous to suggest malignancy in and of them. Earlier biopsy of small breast cancers will be prompted in these situations by indicating more definitively the presence of truly suspicious lesions. Even if there is a definitive indication for biopsy of malignant mammographic features seen on 2D mammography, not infrequently, otherwise unsuspected multicentric foci of the tumor can only be identified with breast tomosynthesis. For specific patients, the ability of breast tomosynthesis to more accurately delineate tumor size and the extent of disease will be useful in determining whether excisional biopsy followed by comprehensive radiation therapy indeed represents an acceptable alternative. It must be remembered that there are many potentially fruitful lines of breast tomosynthesis research and development that have not yet begun to be explored. It will be many years before breast tomosynthesis is fully evaluated. Current clinical research has addressed the importance of this imaging modality in its capability to detect and diagnose breast cancer earlier.

8.3 Work-up and follow-up studies

Follow-up and especially breast biopsy is never cost effective. The cost is enormous in terms of emotional and physical trauma for the woman undergoing the procedure and anguish for the family. The financial cost is also tremendous[26, 56, 93]. Another topic for discussion has been whether or not the biopsy procedure in itself has deleterious effects on the course of the disease. An excisional biopsy or even a needle biopsy may theoretically promote tumor cell spread locally or distantly via opened blood and lymph vessels. However, by doing a complete removal of the tumor for biopsy purposes this problem may be solved. There is almost universal agreement among most surgeons that ablative mammary procedures should not be undertaken unless malignancy has been verified by microscopic examinations[124]. Of course the value of any examination may be measured by three major criteria: its ability to either confirm a suspected diagnosis or exclude the abnormality, its associated risk, discomfort, or inconvenience and its cost[11]. To be clinically successful, new methods of breast imaging must offer improvement over existing methods in increased sensitivity or specificity.

8.4 Radiation dose

The radiation dose delivered to the breast through mammography has found renewed interest with the introduction and compliance of breast cancer screening and with required quality assurance standards. Radiation exposure not only depends on the x-ray beam quality, breast thickness and composition, but also on the particular components of the imaging system. The numerical dose value is also determined by the dose quantity used for describing the radiation exposure. The risk/benefit analyses carried out during the last few years demonstrated that the benefit of mammography significantly exceeds the radiation risk in women age 40 or even at age 35. It should be pointed out, however, that the reduction of breast cancer mortality due to mammographic screening may vary between screening programs and may be restricted to women of age 50 years and over[115]. The tomosynthesis sequence in screening is performed at

approximately 1-1.5 times the radiation dose of a conventional mammogram. When performing the 3D study with diagnostic tomosynthesis, the dose is not such a limiting factor. Breast cancer detection and diagnosis is a demanding procedure. There is no perfect method, all have advantages and disadvantages even under optimal conditions. In order to avoid unnecessary recalls and anxiety, the mammography examination should be complete, thorough and preferably reported before releasing the patient. There are no pathognomonic mammographic signs of malignancy. There are benign lesions that are indistinguishable from malignancy, but fortunately they are not common. The variations and settings of both of these signs, separately and in combination, are numerous. This is an opportunity that should be pursued with vigor[74].

8.5 Future of breast tomosynthesis clinical trials

In planning breast tomosynthesis trials we should take note of what has already been learned from the randomized trials of breast cancer screening with conventional 2D mammography. It is important to focus on trials designs, potential shortcomings of the trial and associated risks if any. Two important elements related to the potential effectiveness of screening are the sensitivity of the screening test and the mean sojourn time. The latter is the average duration of the preclinical screen-detectable phase, which is the window of opportunity for early detection. Over diagnosis is usually defined as the proportion of cases confirmed as cancers, diagnosed during a screening program that would not have come to clinical attention if screening had not taken place. The main risks and other adverse consequences from existing 2D mammography screening include pain and discomfort from breast compression, patient experienced anxiety due to recall for additional imaging, and false-positive biopsies. Radiation risk, even for multiple screenings, is negligible at current mammography doses[110]. High-risk breast lesions are ductal and lobular proliferations that have been shown to have either a statistical association with increased risk of subsequent breast cancer, or genetic alterations or mutations similar to those present in ductal carcinoma in situ (DCIS), or infiltrating carcinoma of the breast. The presence of these genetic alterations suggests that proliferations, such as atypical ductal hyperplasia (ADH), are actually an evolving clonal precursor lesion that already contains one or more of the mutations that distinguish neoplastic lesions, such as DSIS, from benign hyperplasia. Indeed, it is becoming increasingly evident that those lesions associated with increased statistical risk do have some of the mutations that have been identified in recognized types of carcinoma. For example, proliferative breast disease, such as typical hyperplasia, has a 1.5 times relative risk, whereas typical hyperplasia associated with radial scar formation has a 3 times relative risk[102]. This thesis demonstrated that tomosynthesis is capable of detecting slight distortions in breast tissue which were associated with ADH, radial scar, and DCIS.

As stated before, breast tomosynthesis shows promise of better breast cancer detection and diagnosis, even though there are many challenges in technology and clinical performance that lie ahead. Breast tomosynthesis needs clinical acceptance in order to play a successful role in breast cancer detection, diagnosis and treatment. In order to gain clinical acceptance a number of trials must be conducted which provide conclusive evidence that breast tomosynthesis screening is associated with a significant reduction in breast cancer mortality. Screening and diagnostic breast tomosynthesis trials have achieved good results with an

acceptable increase in specificity and sensitivity for detecting and diagnosing challenging breast cancer cases. The goal of breast tomosynthesis is the detection of a high percentage of early stage breast cancers while maintaining an acceptable recall rate, biopsy rate and biopsy yield. The first measure is sensitivity, which assesses the ability of radiologists to detect breast cancer on mammography, should be better than 85%. Follow-up on all cases, both positive and negative ones, is necessary to determine sensitivity accurately[14, 20]. Although the primary role of the radiologist is to detect early breast cancers, it is also important to have an acceptable recall rate. In mammography, the term 'false-positive' can be used to refer to two situations: recall for evaluation when cancer is not present or a biopsy recommendation for which benign disease is found. The number of false-positives should be as low as possible, without significantly reducing the breast cancer detection rate[8, 19, 20, 39, 47, 65, 101]. Ideally the recall-rate should be less than 10%. Less than 1% of screening cases should lead to biopsy, and of those cases, the positive biopsy yield should be greater than 25%[14, 20]. There are many challenges in tomosynthesis as well as conventional 2D mammography. There is increased demand, inadequate staffing, high patient expectations, and excessive costs for providing services[20] utilizing new technologies and modalities in breast care. This requires teamwork; the radiologists, physicists, surgeons, technologists, administrators, equipment manufactures all have key roles to play. Breast tomosynthesis is one of the most challenging areas today, but it is also one of the most rewarding, with a significant impact on cancer mortality and the nation's public health.

REFERENCES

1. Alvarez RE, Macovski A. Energy-selective reconstructions in x-ray computerized tomography. Phys Med Biol 1976;21:733-744.
2. Baily NA, Lasser EC, Crepeau RL. Electrofluoroplanigraphy. Radiol 1973;107:669 671.
3. Bassett LW, Kimme-Smith C. Breast sonography. AJR Am J Roentgenol 1991; 156:449-455.
4. Berg JW. Clinical implications of risk factors for breast cancer. Cancer 1984;53: 589-591.
5. Boone JM. Breast CT: Its prospect for breast cancer screening and diagnosis. RSNA Categorial Course in Diagnostic Radiology Physics: Advances in Breast Imaging-Physics, Technology, and Clinical Applications 2004;165-177.
6. Boone JM. Spectral modeling and compilation of quantum fluence in radiography and mammography. Proc SPIE 1998;3336:592-601.
7. Boone JM, Nelson TR, Lindfors KK, Seibert JA. Dedicated breast CT: radiation dose and image quality evaluation. Radiology 2001;221:657-667.
8. Brett J, Austoker J. Women who are recalled for further investigation for breast cancer screening: psychological consequences 3 years after recall and factors affecting re-attendance. J Pub Health Med 2001;23:292-300.
9. Båth M. Imaging properties of digital radiographic systems: Development, application, and assessment of evaluation methods based on linear-systems theory. Doctoral Thesis of Department of Radiation Physics, Göteborg University 2003.
10. Carson PL, LeCarpentier GL, Roubidoux MA, Erkamp RQ, Fowlkes JB, Goodsitt MM. Physics and technology of breast US imaging including automated three-dimensional US. RSNA Categorial Course in Diagnostic Radiology Physics: Advances in Breast Imaging-Physics, Technology, and Clinical Applications 2004; 223-232.
11. Christopher RB. Future of breast imaging: Potential role of digital mammography, Doppler US, and transillumination. RSNA categorial course in diagnostic radiology breast imaging 1986;16:91-92.
12. Cunnigham. Applied linear-systems theory. Handbook of Medical Imaging: Physics and Psychophysics 2000;1:79-159.
13. Dobbins JT, Warp RJ. Dual-energy methods for tissue discrimination in chest radiography. Advances in Digital Radiography: RSNA Categorial Course in Diagnostic Radiology Physics 2003;173-179.
14. D'Orsi CJ, Bassett LW, Berg WA, Feig SA, Jackson VP, Kopans DB, et al. Breast imaging reporting and data system. American College of Radiology 2003.
15. Duffy SW, Tabar L, Vitak B, et al. The Swedish two-county trial of mammographic screening: cluster randomisation and end point evaluation. Ann Oncol 2003; 14:1196-1198.
16. Dupont WD, Page DL. Risk factors for breast cancer in women with proliferative breast disease. N Engl J Med 1985;312:146-151.

17. Durfee SM, Selland DLG, Smith DN, et al. Sonographic evaluation of clinically palpable breast cancers invisible on mammography. The Breast Journal 2000;6:247-251.
18. Elliott G, Starkings S. The use of spreadsheets for teaching statistics at degree level. Proc The fourth international conference on teaching statistics 1994;1:140.
19. Elmore JG, Barton MB, Moceri VM, Polk S, Arena PJ, Fletcher SW. Ten-year risk of false positive screening mammograms and clinical breast examination. N Engl J Med 1998;338:1089-1096.
20. Farria DM, Monsees B. Screening mammography practise essentials. Radiol Clin N Am 2004;42:831-843.
21. Feig SA. Adverse effects of screening mammography. Radiol Clin N Am 2004; 42:807-819.
22. Fischer U, Kopka L, Grabbe E. Breast carcinoma: effect of pre-operative contrast-enhanced MR imaging on the therapeutic approach. Radiology 1999;213: 881-888.
23. Fletcher SW, Black W, Harris R, Rimer BK, Shapiro S. Report of the international Workshop on screening for Breast Cancer. J Natl Cancer Inst 1993;85:1644-1656.
24. Frazier TG, Murphy JT, Furlong A. The selected use of ultrasound mammography to improve diagnostic accuracy in carcinoma of the breast. J Surg Oncol 1985; 29:231-232.
25. Fujita H, Tsai D, Itoh T, doi K, Morishita J, Ueda K, Ohtsusuka A. A simple method for determining the modulation transfer function in digital mammography. IEEE Transactions on Medical Imaging 1992;11:34-39.
26. Galkin BM, Feig SA, Patchefsky AS, Muir HD. Elemental analysis of breast calcifications. Recent results in cencer research: Breast cancer 1987;105: 89-94.
27. Gatti GG, Harwell M. Advantages of computer programs over power charts for the estimation of power. Journal of Statistics Education 1998;6:3.
28. Glick SJ, Vedantham S, Karellas A, A'Hern RP. Investigation of optimal kVp settings for CT mammography using a flat panel imager. SPIE Proc 2002;4682:392-402.
29. Gordon PB. Ultrasound for breast cancer screening and staging. Radiol Clin N Am 2002;40:431-441.
30. Grant DG. Tomosynthesis: a three-dimensional radiographic imaging technique. IEEE Trans Biomed Eng 1972;19:20-28.
31. Hackshaw A. EUSOMA review of mammography screening. Ann Oncol 2003; 14:1193-1195.
32. Hall AG. A workshop approach using spreadsheets for the teaching of statistics and probability. Computers and Educations 1995;25:5-12.
33. Harms SE, Flamig DP, Helsey KL, et al. MR imaging of the breast with rotating delivery of excitation off resonance clinical experience with pathologic correlation. Radiology 1994;190:485-493.
34. Hendrick RE. Physics and technical aspects of breast MR imaging. RSNA Categorial Course in Diagnostic Radiology Physics: Advances in Breast Imaging-Physics, Technology, and Clinical Applications 2004;259-278.
35. Hendrick RE, Haake EM. Basic physics of contrast agents and maximization of image contrast. J Magn Reson Imaging 1993;3:137-148.

36. Heywang S, Wolf A, Pruss E, at al. MR imaging of the breast with Gd-DTPA: Use and limitations. Radiology 1989;171:95-103.
37. Heywang-Köbrunner S. Contrast-enahnced magnetic resonance imaging of the breast. Investigative Radiology 1994;29:94-104.
38. Hunt N. Teaching statistics using a spreadsheet. Proc The fourth international conference on teaching statistics 1994;2:432.
39. Hunt KA, Rosen EL, Sickles EA. Outcome analysis of imaging annual versus biennial screening mammography: a review of 24,211 examinations. AJR Am J Roentgenol 1999;173:285-289.
40. Ishigaki T, Sakuma S, Ikeda M. One-shot dual-energy subtraction chest imaging with computed radiography: clinical evaluation of film images. Radiology 1988;168: 67-72.
41. Jackson VP. The role of US in breast imaging. Radiology 1990; 177:3051.
42. Jackson VP, Hendrick RE, Feig SA, Kopans DB. Imaging of the radiologically dense breast. Radiology 1993;188:297-301.
43. Jacobs MA, Barker PB, Bottomley PA, et al. Proton magnetic resonance spectroscopic imaging of human breast cancer: a preliminary study. J Magn Reson Imaging 2004;19:68-75.
44. Joe BN, Bae KT, Chen VY, et al. Dynamic MR contrast enhancement characteristics of breast cancer: effect of contrast injection rate (abstr.). Radiology 2003;229(P): 289.
45. Jong RA, Yaffe MJ, Skarpathiotakis M, et al. Contrast enhanced digital mammography: initial clinical experience. Radiology 2003; 228:842-850.
46. Kaiser WA, Zeitler E. MR imaging of the breast: fast imaging sequency with and without Gd-DTPA preliminary observations. Radiology 1989;170:639-649.
47. Kan L, Olivotto IA, Sickles EA, Coldman AJ. Standardized abnormal interpretation and cancer detection ratios to assess reading volume and reader performance in a breast screening performance in a breast program. Radiology 2000;215:563-567.
48. Kelcz F, Zink FE, Peppler WW, Kruger DG, Ergun Dl, Mistretta CA. Conventional chest radiography vs. dual-energy computed radiography in the detection and characterization of pulmonary nodules. AJR Am J Roentgenol 1994;162:271-278.
49. Kopans DB. Digital mammography: Principles, equipment, technique and clinical results. Breast Imaging: RSNA Categorial course in Diagnostic Radiology 2005;77-82.
50. Kopans DB, Swann CA, White G, McCarthy KA, Hall DA. Significance of mammographically detected asymmetric tissue density. Radiology 1987;165(P): 120.
51. Krufer DG, Zink F, Peppler WW, Ergun DL, Mistretta CA. A regional convolution kernel algorithm for scatter correction in dual-energy images: comparison to single-kernel algorithms. Med Phys 1994;21:175-184.
52. Kuhl CK, Mielcarek P, Klaschik S, et al. Dynamic breast MR imaging: are signal intensity time course data useful for differential diagnosis of enhancing lesions? Radiology 1999;211:101-110.

53. Lazzari B, Giacomo B, Cesare G, Nykänen K. Physical characteristics of a clinical prototype for full-field digital mammography with *a*-Se flat panel detector. SPIE Proc 2003;5030:656-666.
54. Lee DL, Cheung LK, Rodricks B, Powell GF. Improved imaging performance of a 14x17-inch direct radiography™ system using Se/TFT detector. Proc SPIE 1998;3336:14-23.
55. Lehtimäki M, Nelson M, Lechner M, Elvecrog E. Improved method for diagnosis in clinical mammography with breast tomosynthesis. Internatiol Workshop on Digital Mammography (IWDM) 2004.
56. Lehtimäki M, Pamilo M. Clinical aspects of diagnostic 3-dimensional mammography. Seminars in Breast Disease 2004;6:72-77.
57. Lehtimäki M, Pamilo M, Raulisto L, Kalke M, First clinical results with real-time selenium-based full-field digital mammography 3D imaging system. SPIE Proc 2004;5368:922-929.
58. Lehtimäki M, Pamilo M, Raulisto L, Roiha M, Kalke M, Siltanen S, and Ihamäki T. Diagnostic clinical benefits of digital spot and digital 3D mammography following analysis of screening findings. SPIE Proc 2003;5029:698-706.
59. Lemacks MR, Kappadath SC, Shaw CC, Liu X, Whitman GJ. A dual-energy subtraction technique for microcalcification imaging in digital mammography: a signal-to-noise analysis. Med Phys 2002;29:1739-1751.
60. Lewin JM, D'Orsi CJ, Hendrick RE. Digital mammography. Radiol Clin N Am 2004;42:871-884.
61. Lewin JM, D'Orsi CJ, Hendrick RE, Moss LJ, Isaacs PK, Karellas A, et al. Clinical comparison of full-field digital mammography to screen-film mammography for breast cancer detection. AJR Am J Roentgenol 2002;179:671-677.
62. Lewin JM, Hendrick RE, D'Orsi CJ, Isaacs PK, Moss LJ, Karellas A, et al. Comparison full-field digital mammography to screen-film mammography for cancer detection: results of 4945 paired examinations. Radiology 2001;218:873-880.
63. Lewin JM, Isaacs PK, Vance V, Larke FJ. Dual-energy contrast-enhanced digital subtraction mammography: feasibility. Radiology 2003;229:261-268.
64. Liberman L, Morris EA, Kim CM, et al. MR imaging findings in the contralateral breast of women with recently diagnosed breast cancer. AJR Am J Roentgenol 2003;180:333-341.
65. Linver MN, Paster SB. Mammography outcomes in a practice setting by age: prognostic factors, sensitivity, and positive biopsy rate. J Natl Cancer Inst 1997;22: 113-117.
66. Linver MN; Paster SB, Rosenberg RD, Key CR, Stidley CA, King WV. Improvement in mammography interpretation skills a community radiology practise after dedicated teaching courses: 2-year medical audit of 38,633 cases. Radiology 1992;184:39-43.
67. Loustauneau V, Bissonnette M, Cadieux S, Hansroul M, Masson E, Savard S, Polischuk B, Ghosting comparison for large-area selenium detectors suitable for mammography and general radiography. SPIE Proc 2004;5368:162-169.

68. Loustauneau V, Bissonnette M, Cadieux S, Hansroul M, Masson E, Savard S, Polischuk B, Lehtimäki M. Imaging performance of a clinical selenium flat-panel detector for advanced applications in full-field digital mammography. SPIE Proc 2003;5030:1010-1020.
69. Ludbrook J. Microcomputer statistics packages for biomedical scientists. Clinical and Experimental pharmacology and Physiology 1995;12:976-986.
70. Mandelkorn F, Stark H. Computerized tomosynthesis, stereoscopy, and coded-scan tomography. Applied Optics 1979;17:175-180.
71. Maravilla KR, Murry RC Jr, Horner S. Digital tomosynthesis: technique for electronic reconstructive tomography. Am J Radiol 1983;141:497-502.
72. Mayer-Ebrecht D, Weiss H. Tomosynthesis – three dimensional x-ray imaging by means of holography or electronics. Optica Acta 1977;24:293-303.
73. McCauley TG, Stewart AX, Stanton MJ, Wu T, Philips WC. Three dimensional breast image reconstruction from a limited number of views. SPIE Proc 2000;3977: 384-395.
74. McLelland. Earlier detection of breast cancer: an overview. Recent results in cancer research: Advances in breast cancer detection 1990;119:10-17.
75. McLelland. Stellate lesion of the breast. Recent results in cancer research: Advances in breast cancer detection 1990;119:24-28.
76. Miller ER, McCurry EM, Hruska B. An infinite number of laminagrams from a finite number of radiographs. Radiol 1971;98:249-255.
77. Nash JC, Quon TK. Issues in teaching statistical thinking with spreadsheets. Journal of Statistics Education 1996;4:1.
78. Newstead GM. Clinical role of breast MR imaging. Physics and technology of breast US imaging including automated three-dimensional US. RSNA Categorial Course in Diagnostic Radiology Physics: Advances in Breast Imaging-Physics, Technology, and Clinical Applications 2004; 279-289.
79. Niklason LT, Christian BT, Niklason LT, et al. Digital tomosynthesis in breast imaging. Radiology 1997;205:399-406.
80. Niklason L, Niklason L, Kopans DB. Tomosynthesis system for breast imaging. U.S. Patent 5,872,828, 1999.
81. Ning R, Chen B, Conover D, Mchuhg L, Cullinan J, Yu R. Flat panel detector-based cone beam volume CT mammography imaging: preliminary phantom study. SPIE Proc 2001:4320:601-610.
82. Nishikawa RM, Mawdsley GE, Fenster A, Yaffe MJ. Scanned-projection digital mammography. Med Phys 1987;14(5):717-727.
83. Nystrom L, Rutqvist LE, Wall S, et al. Breast cancer screening with mammography: overview of Swedish randomised trials. Lancet 1993;341:973-978.
84. Orel SG, Schnall MD, LiVolsi Va, et al. Suspicious breast lesions: MR imaging with radiology-pathologic correlation. Radiology 1994;190:485-493.
85. Overdick M, Solf T, Wischmann H. Temporal artifacts in flat dynamic x-ray detectors. Proc SPIE 1998;3336:47-58.

86. Pisano ED, Gatsonis C, Hendrick E, Yaffe M, Baum JK, Acharyya S, Conant EF, Fajardo LL, Bassett L, D'Orsi C, Jong R, Rebner M. Diagnostic performance of digital versus film mammography for breast cancer screening. The New England Journal of Medicine 2005;353(17):1773-1783.
87. Polack SP, Tosteson AN, Grove Mr, Wells WA, Carney PA. Mammography in 53,803 women from the New Hampshire mammography network. Radiology 2000;217:832-840.
88. Polischuk B, Savard S, Loustauneau V, Hansroul M, Cadieux S, Vagué A. Se-based-flat-panel detector for screening mammography. SPIE Proc 2001;4320:582-589.
89. Rafferty EA. Breast tomosynthesis. Advances in Digital Radiography: RSNA Categorical Course in Diagnostic Radiology Physics 2003;219-226.
90. Rafferty EA, Georgian-Smith D, Kopans DB, McCarthy KA, Hall DA, Moore R, Wu T. Comparison of full-field digital tomosynthesis with two view conventional film screen mammography in the prediction of lesion malignancy (abstr.). Radiology 2002;225(P):268.
91. Raffery EA, Georgian-Smith D, Kopans DB, Wu T, Moore R. Eliminating the fake out: comparison of conventional two view film screen mammography with full field-digital tomosynthesis in distinguishing mammographic abnormalities from superimposition of normal breast structures (abstr.). Radiology 2002;225(P):682.
92. Rafferty EA, Kopans DB, Georgian-Smith D, Hall DA, Wu T. Evaluation of the call-back rate for screening mammography using full-field digital tomosynthesis versus conventional film screen mammography (abstr.). AJR Am J Rontgenol 2003;180 Suppl:S75.
93. Rafferty EA, Kopans DB, Wu T, Mooore RH. Breast tomosynthesis: will a single view do? (abstr.). In Radiological Society of North America scientific assembly and annual meeting program. Oak Brook, Il; Radiological Society of North America 2004;567.
94. Rafferty EA, Wu T, Moore RH, Yeh ED, Staffa MM, Kopans DB. Optimization of image acquisition and display algorithm to enhance visualization of microcalcifications during digital breast tomosynthesis (abstr.). Radiology 2003;229(P):423-424.
95. Reinikainen H. Complementary imaging of solid breast lesions. Contribution of ultrasonography, fine-needle aspiration biopsy, and high-field and low-field MR imaging. Doctoral Thesis of Acta Univ Oul D 734 2003.
96. Rosenberg RD, Hunt WC, Williamson MR, et al. Effects of age, breast density, ethnicity, and estrogen replacement therapy on screening mammographic sensitivity and cencer stage at diagnostic: review of 183,134 screening mammograms in Albuquerque, New Mexico. Radiology 1998; 209:511-518.
97. Ruttimann UE, Groenhuis RAJ, Webber RL. Computer tomosynthesis: a versatile three-dimensional imaging technique. 7th annual symposium on computer applications in medical care Proc 1983:783-786.
98. Sadowsky N, Kopans DB. Breast cancer. Radiol Clin North Am 1983;21:51-80.
99. Samei E. Performance of digital radiographic detectors: Quantification and assessment methods. Advances in Digital Radiography: RSNA Categorial Course in Diagnostic Radiology Physics 2003;37-47.

100. Samei E, Tornai MP. Optimizing beam quality for x-ray computed mammotomography. SPIE Proc 2003;5030:575-584.
101. Schwartz LM, Woloshin S, Fowler FJ, Welch HG. Enthusiasm for cancer screening in the United States. JAMA 2004;291:71-78.
102. Sewell CW. Pathology of high-risk breast lesions and ductal carcinoma in situ. Radiol clin N Am 2004;42:821-830.
103. Shtern F. Digital mammography and related technologies: a perspective from the National Cancer Institute. Radiology 1989; 171:87-90.
104. Sickles EA. Breast calcifications: mammographic evaluation. Radiology 1986;160: 289-293.
105. Sickles EA. Mammographic features of 'early' breast cancer. Am J Roentgenol 1984;143:461-464.
106. Sickles EA. Mammographic features of malignancy found during screening. Recent results in cancer research: Advances in breast cancer detection 1990;119:88-93.
107. Siewerdson JH, Jaffray DA. A ghost story: spatio-temporal response characteristics of an indirect-detector flat-panel images. Med Phys 1999;26:1624-1641.
108. Skaane P, Young K, Skjennald A. Population-based mammography screening: comparison of screen-film and full-field digital mammography with soft-copy reading – Oslo I study. Radiology 2003;229:877-884.
109. Skarpathiotakis M, Yaffe MJ, Bloomquist AK, et al. Development of CDM. Med Phys 2002;29:2419-2426.
110. Smith RA, Duffy SW, Gabe R, Tabar L, Yen AMF, Chen THH. The randomized trials of breast cancer screening: what have we learned? Radiol Clin N Am 2004;42: 793-806.
111. Sommer FG, Brody WR, Gross D, Macovski A. Renal imaging with dual-energy projection radiography. ALR Am J Roentgenol 1982;138:317-322.
112. Sone S, Kasuga T, Sakai F, et al. Chest imaging with dual-energy subtraction digital tomosynthesis. Acta Radiol 1993;34:346-350.
113. Stack JP, Redmond OM, Codd MB, Dervan PA, Ennis JT. Breast disease: tissue characterization with Gd-DTPA enhancement profiles. Radiology 1990;174:95-103.
114. Suryanarayanan S, Karellas A, Vedantham S, ed H, Baker SP, D'Orsi CJ. Flat-panel digital mammography system: contrast-detail comparison between screen-film radiographs amd hard-copy images. Radiology 2002;225(3):801-807.
115. Säbel M. Radiation exposure. The practice of mammography. Pathology-Technique-Interpretation-Adjunct Modalities 2002;1:92-95.
116. Tabar L, Yen MG, Vitak B, Chen HH, Smith RA, Duffy SW. Mammography service screening and mortality in breast cancer patients: 20-year follow-up before and after introduction of screening. Lancet 2003;361:1405-1410.
117. Tabar L, Duffy SW, Yen MF, et al. All-cause mortality among breast cancer patients in a screening trial: support for breast cancer mortality as an end point. J Med Screen 2002;9:159-162.
118. Tabar L, Fagerberg G, Duffy SW. Update of the Swedish two-county program of mammographic screening for breast cancer. Radiol Clin North Am 1992;30:187-210.

119. Tornai MP, Bowsher JE, Jaszczak RJ, et al. Mammotomography with pinhole incomplete circular orbit SPECT. J Nucl Med 2003;44:583-593.
120. Tousignant O, Choquette M, Demers Y, Laperriere L, Leboeuf J, Honda M, Nishiki M, Takahashi A, and Tsukamoto A. Progress report on the performance of real-time selenium flat-panel detectors for direct x-ray imaging. SPIE Proc 2002;4692:503-510.
121. Varjonen M, Pamilo M, Raulisto L. Clinical benefits of combined three-dimensional digital breast tomosynthesis and ultrasound imaging. SPIE Proc 2005;5745:562-571.
122. Vedula AA, Glick SJ, Gong X. Computer stimulation of CT mammogtaphy using a flat-panel images. SPIE Proc 2003;5030:349-360.
123. Warp RJ, Dobbins JT III. Quantative evaluation of noise reduction strategies in dual-energy imaging. Med Phys 2003;30:190-198.
124. Watt-Boolsen S, Blichert-Toft M, Andersen JA, Andersen KW. Changing aspects of biopsy of the breast: Is breast biopsy a prognostic hazard? Recent results in cencer research: Breast cancer 1987;105:97-105.
125. Webber RL, Self-calibrated tomosynthetic, radiographic-imaging system, method and device, US patent 5,359,637, 1994.
126. Webber RL, Self-calibrated tomosynthetic, radiographic-imaging system, method and device, US patent 5,668,844, 1997.
127. Webber RL, Bettermann W. A method for correcting for errors produced by variable magnification in three-dimensional tuned-aperture computed tomography. Dentomaxillofac Radiol 1999;28:305-310.
128. Webber RL, Hemler PF, Lavery J. Objective evaluation of linear and nonlinear tomosynthetic reconstruction algorithms. SPIE Proc 2000;3981:224-231.
129. Webber RL, Horton RA, Tyndall DA. Tuned-aperture computed tomography (TACT®). Theory and application for three-dimensional dento-alveolar imaging. Dentomaxillofac Radiol 1997;26:53-62.
130. Webber RL, Horton RA, Underhill TE, Ludlow JB, Tyndall DA: Comparison of film, direct digital, and tuned-aperture computed tomography (TACT) images for identifying the location of crestal effects around endosseous titanium implants. Oral Surg Oral Med Oral Pathol Oral Radiol Endod 1996;81:480-490.
131. Webber RL, Hunter RU, Freimanis RI. A controlled evaluation of tuned-aperture computed tomography applied to digital spot mammography. Journal of digital imaging 2000;13:90-97.
132. Webber RL, Messura JK. An in vivo comparison of diagnostic information obtained from tuned-aperture computed tomography and conventional dental radiographic imaging modalities. Oral Surg Oral Med Oral Pathol Oral Radiol Endod 1999;88: 239-247.
133. Webber RL, Underhill PF, Hemler PF, Lavery J. A nonlinear algorithm for task-specific tomosynthetic image reconstruction. SPIE Proc 1999;3659:258-265.
134. Weidner N, Semple JP, Welch WR, et al. Tumor angiogenesis and metastasis correlation in invasive breast carcinoma. N Engl J Med 1991;324:1-7.
135. Weinreb JC, Newstead G. MR imaging of the breast. Radiology 1995;196:593-610.
136. Wu T, Zhang JM, Moore RH. Digital tomosynthesis mammography using a parallel maximum likelihood reconstruction method. SPIE Proc 2004;5368:1-11.

137. Wu T, Moore RH, Raffery EA, Kopans DB. Breast tomosynthesis: Methods and applications. Categorial Course in Diagnostic Radiology Physics: Advances in Breast Imaging-Physics, Technology, and Clinical Applications 2004;149-163
138. Yaffe MJ. Physics of digital mammography. Digital mammography 2004: 4-14.
139. Yorkston J. Digital radiography technology. Advances in Digital Radiography: RSNA Categorial Course in Diagnostic Radiology Physics 2003;23-36.
140. Ziedses des Plantes BG. Selected works of BG Ziedses des Planted. Excerpta Medica 1973:137-140.

APPENDIX

DIGITAL BREAST TOMOSYNTHESIS
Evaluation Form

Patient Name (or patient code)	Radiologist (name or code)

Detailed Lesion Description – Mammography (M)

Lesion Shape:

☐ Round	☐ Oval	☐ Other _____
☐ Lobulated	☐ Spiculated Shape	
☐ Irregular	☐ Architectural Distortion	
☐ Asymmetric Density		

Calcifications:

☐ Benign-appearing	☐ Other Comments _____
☐ Suspicious	
☐ Indeterminate	

Lesion Shape:

☐ Circumscribed	☐ Spiculated	☐ Other _____
☐ Microlobulated		
☐ Obscured		
☐ Ill-defined		

Assessment - MAMMOGRAPHY

- ☐ 1 Negative
- ☐ 2 Benign
- ☐ 3 Probably Benign
- ☐ 4 Suspicious Abnormality
- ☐ 5 Malignant Highly Suggestive of Malignancy

Notes:

Detailed Lesion Description – Ultrasound (US)

Findings:

☐ Simple cyst ☐ Normal parenchyma ☐ Other _____
☐ Complex lesion ☐ Dilated duct
☐ Solid mass ☐ Not visible
☐ Indeterminate

Lesion Shape:

☐ Oval ☐ Micro lobulations ☐ Other _____
☐ Less than 3 gentle lobulations ☐ Taller than wide
☐ More than 3 gentle lobulations
☐ Angular

Correlates with:

☐ Mammographic findings ☐ Other Comments _____
☐ Palpable findings
☐ Mammographic and palpable findings

Echo Texture:

☐ Hypoechoic ☐ Anechoic ☐ Other _____
☐ Isoechoic
☐ Hyperechoic
☐ Heterogeneous

Assessment - ULTRASOUND

☐ 1 Negative
☐ 2 Benign
☐ 3 Probably Benign
☐ 4 Suspicious Abnormality
☐ 5 Malignant Highly Suggestive of Malignancy

Notes:

Detailed Lesion Description – Digital Breast Tomosynthesis (DBT)

Lesion Shape:

☐ Round ☐ Oval ☐ Other _____
☐ Lobulated ☐ Spiculated Shape
☐ Irregular ☐ Architectural Distortion
☐ Asymmetric Density

Calcifications:

☐ Benign-appearing ☐ Other Comments _____
☐ Suspicious
☐ Indeterminate

Lesion Shape:

☐ Circumscribed ☐ Spiculated ☐ Other _____
☐ Microlobulated
☐ Obscured
☐ Ill-defined

Correlates with:

☐ Mammographic findings ☐ Other Comments _____
☐ Palpable findings
☐ US findings

Assessment – DIGITAL BREAST TOMOSYNTHESIS

☐ 1 Negative
☐ 2 Benign
☐ 3 Probably Benign
☐ 4 Suspicious Abnormality
☐ 5 Malignant Highly Suggestive of Malignancy

Notes:

FINAL Assessment **(INVASIVE PROCEDURES INCLUDED)**
☐ Normal
☐ Benign
☐ Early recall
☐ Surgically proven benign
☐ Non-invasive cancer
☐ Invasive cancer
☐ Biopsy Result _____
☐ Surgical Pathology Report _____
☐ Other information _____

FINAL Assessment based on
☐ ULTRASOUND (US)
☐ MAMMOGRAPHY (M)
☐ US + M
☐ DIGITAL BREAST TOMOSYNTHESIS (DBT)
☐ DBT + US
☐ DBT + US + M
☐ DTB + M
☐ Other _____

COMPARISON:

SPICULATED ILL-DEFINED LESIONS:		**MASSES WITH REGULAR BORDERS:**	
SPICULATION IS SEEN BETTER WITH DBT	EXTENSION (INFILTRATION) TO SURROUNDING TISSUES ARE SEEN BETTER WITH DBT	THE CONTOURS WITH DBT ARE	EXTENSION (INFILTRATION) TO SURROUNDING TISSUES ARE SEEN BETTER WITH DBT
☐ Yes	☐ Yes	☐ Equal	☐ Yes
☐ May be	☐ May be	☐ Better defined	☐ May be
☐ No	☐ No	☐ Less defined	☐ No
☐ Worst	☐ Worst		☐ Worst

Notes:

ORIGINAL PUBLICATIONS

Publication I

Lehtimäki M, Pamilo M

Clinical aspects of diagnostic 3D mammography

Seminars in Breast Disease, 2003; 6(2): 72-77.

Publication II

Lehtimäki M, Pamilo M, Raulisto L, Roiha M, Kalke M, Siltanen S, Ihamäki T

Evaluation clinique des performances diagnostiques de la mammography numérique avec spot et de la mammography numérique 3D suite au dépistage d'anomalies

Journal de la Société Française de Mastologie et d'Imagerie du Sein, 2003; 13(4): 309-316.

Publication III

Loustauneau V, Bissonnette M, Cadieux S, Hansroul M, Masson E, Savard S, Polischuk B, Lehtimäki M

Imaging performance of a clinical selenium flat-panel detector for advanced applications in full-field digital mammography

Proceedings of SPIE, Vol 5030, 1010-1020, 2003.

Publication IV

Varjonen M, Pamilo M, Raulisto L

Clinical benefits of combined diagnostic three-dimensional digital breast tomosynthesis and ultrasound imaging

Proceedings of SPIE, Vol 5745, 562-571, 2005.

Combining clinical benefits of digital breast tomosynthesis and ultrasound imaging

Breast Cancer Research Journal

Submitted for publication in November 2005. Revised in April 2006.

Publication V

Varjonen M, Pamilo M, Raulisto L

Digital breast tomosynthesis in diagnostic mammography

Emerging Technologies in Breast Imaging and Mammography,

Accepted for publication and to be published in April 2006.

Publication VI

Lehtimäki M, Pamilo M, Raulisto L, Kalke M

First results with real-time selenium-based full-field digital mammography three-dimensional imaging system

Proceedings of SPIE, Vol 5368, 922-929, 2004.

Publication VII

Lehtimäki M, Pamilo M, Raulisto L, Roiha M, Kalke M, Siltanen S, Ihamäki T

Diagnostic clinical benefits of digital spot and digital 3D mammography following analysis of screening findings

Proceedings of SPIE, Vol 5029, 698-706, 2003.

Tampereen teknillinen yliopisto
PL 527
33101 Tampere

Tampere University of Technology
P.O. Box 527
FIN-33101 Tampere, Finland